# 7.2: Description of Sentinel-3 SRAL SAR mode, and new products for GMES land and marine services


Project number
313238

Project title
LOTUS— Preparing Land and Ocean Take Up from Sentinel-3

Call (part) identifier
FP7-SPACE-2012-1

Funding scheme
Collaborative project


Deliverable Number D7.2
Title: “Description of Sentinel-3 SRAL SAR mode, and new products for GMES land and marine services”
Nature: Report
Dissemination level: Public

Status: v2.1
Date: 15th December 2015

| DOCUMENT CHANGE LOG | | | | |
|---|---|---|---|---|
| Rev. | Date | Sections modified | Comments | Changed by |
| 1 | 9th November 2015 | Template, Abstract | | C. Pelloquin |
| 2 | 15th November 2015 | 2.1.2, 3.1.3 | Full content | C.Pelloquin |
| 3 | 1st December | 3.1.2 | Full content | P. Berry |
| 4 | 1st December | 2.1.1 | Full content | T. Moreau |
| 5 | 1st December | 3.1.1 | Full content | K. Nielsen |
| 6 | 14th December | 2.1.3 | Full content | O. Andersen |
| 7 | 15th December | All | Format | C. Pelloquin |

# Table of Content

**1. Abstract ..... 6**

**2. Copernicus Marine Service ..... 7**

*2.1. Major improvements ..... 7*

2.1.1. Open Ocean ..... 7

2.1.1.1. Major improvements using SAR altimetry ..... 7

2.1.1.2. Assessment ..... 8

2.1.1.3. Limitations ..... 12

2.1.1.4. Products ..... 13

2.1.2. Costal area ..... 14

2.1.2.1. Major improvements using SAR altimetry ..... 14

2.1.2.2. Assessment ..... 17

2.1.2.1. Limitations ..... 17

2.1.2.2. Products ..... 19

2.1.3. Polar Ocean ..... 20

2.1.3.1. Major improvements using SAR altimetry ..... 20

2.1.3.2. Assessment ..... 21

2.1.3.3. Limitations ..... 22

2.1.3.4. Products ..... 23

*2.2. Recommendations ..... 23*

2.2.1. Open ocean ..... 23

2.2.2. Coastal area ..... 24

2.2.3. Polar ocean ..... 24

**3. Copernicus Land Service ..... 25**

*3.1. Major improvements ..... 25*

3.1.1. River and lakes ..... 25

3.1.1.1. Major improvements using SAR altimetry ..... 25

3.1.1.2. Assessment ..... 26

3.1.1.1. Products ..... 27

3.1.2. Soil moisture ..... 28

3.1.2.1. Major improvements using SAR altimetry ..... 28

3.1.2.2. Assessment ..... 33

3.1.2.3. Assumptions and limitations ..... 35

3.1.2.4. Product Structure and Content ..... 35

3.1.3. Snow depth ..... 37

3.1.3.1. Major improvements using SAR altimetry ..... 37

3.1.3.2. Products ..... 41

*3.2. Recommendations ..... 41*

3.2.1. River and lakes ..... 41

3.2.2. Soil moisture ..... 41

3.2.3. Snow depth ..... 42

**4. Reference ..... 43**

# Table of Figure

*Figure 1 - Power spectral density for SAR-mode and PLRM Sea Level Anomaly ..... 9*

*Figure 2 - Power spectral density for SAR-mode and PLRM sigma-0 ..... 9*

*Figure 3 - Maps of difference between PLRM and SAR Sea Level Anomaly ..... 10*

*Figure 4 - Difference between PLRM and SAR range as function of waves ..... 10*

*Figure 5 - Maps of difference between PLRM and SAR significant wave height ..... 11*

*Figure 6 - Difference between PLRM and SAR significant wave height as function of waves ..... 11*

*Figure 7 - Maps of difference between PLRM and SAR sigma-0 ..... 12*

*Figure 8 - Difference between PLRM and SAR sigma-0 as function of along-track mispointing ..... 12*

*Figure 9 - SAR Altimetry waveforms for satellite track perpendicular to the coast (along track) .. 15*

*Figure 10 - SAR Altimetry waveforms for satellite track parallel to the coast (across track) ..... 16*

*Figure 11 - SAR Altimetry waveforms for satellite track contaminated by land in the across track direction. Location of the track and the studied beam (left). Waveform pre-processed (red point rejected) to be ingested into the SAR waveform retracker (right). ..... 16*

*Figure 12 - Coastal area pre-processing (+ SAMOSA retracker) assessment using as reference CPP retracking solutions. SWH difference along a specific track ..... 17*

*Figure 13 - Coastal area pre-processing (+ SAMOSA retracker) assessment using as reference CPP retracking solutions. SSH difference along a specific track ..... 17*

*Figure 14 - Coastal retracker vs. in-situ SWH (Hs) at Ekofisk, (Central north sea station) ..... 18*

*Figure 15 - Waveform retracking through the coastal retracker. Waveform perturbed by the presence of land in the along-track direction. ..... 18*

*Figure 16 - Waveform retracking through the coastal retracker. Waveform perturbed by the presence of shallow water. ..... 19*

*Figure 17 - The Sentinel-3A tracks in the Polar Ocean. Here around Svalbard. The yellow line at 78.75 is 100 km long and demonstrate that the across track distance at this latitude is around 20 km. ..... 20*

*Figure 18 - Classification in the Arctic Ocean for Sentinel-3 ..... 21*

*Figure 19 - Example of lead detection in area photos from IceBridge co-located Cryosat-2 tracks in the Arctic Ocean in 3013 ..... 21*

*Figure 20 - A total of 34 leads detected by Cryosat-2 (blue) and by the size in the co-located IceBridge area photos. ..... 22*

*Figure 21 - The LOTUS Cryosat-2 daily time series in the Svalbard region and the comparison with monthly sea level data from PSMSL ..... 22*

*Figure 22 - The Svalbard polar ocean region (light blue) and the track polar ocean dataset (red) . 23*

*Figure 23 - Examples of SAR echoes related to inland water bodies ..... 25*

*Figure 24 - (Left) Flow chart describing the steps in SAR retracking procedure. (Right) Flow chart describing the steps in the post-processing ..... 26*

*Figure 25 - Simpson desert DREAM for CryoSat-2 ..... 30*

*Figure 26 - Simpson desert CSME validation soil moisture from Jason2 using enhanced DREAM..... 30*

*Figure 27 - Tenere desert CSME validation dataset from Jason2 using enhanced DREAM ..... 31*

*Figure 28 - Kalahari desert DREAM for CryoSat-2 ..... 31*

*Figure 29 - Kalahari desert CSME validation dataset from Jason2 using enhanced DREAM ..... 32*

*Figure 30 - Cross-calibrated recalculated Cryosat2 SAR mode (red) and LRM (blue) backscatter with underlying DREAM pixels (SAR pink, LRM green)..... 32*

*Figure 31 - Overview of Processing Chain for Sentinel3 Soil Moisture Generation ..... 33*

*Figure 32 - Tenere desert DREAM with Jason2 track locations ..... 34*

*Figure 33 - Soil Moisture product (CSME) validation with Jason2 soil moisture measurements from tracks in Figure 18 (from Berry & Balmbra, 2015b) ..... 34*

*Figure 34 - OCOG width vs snow depth variations ..... 38*

*Figure 35 - Snow depth (up) vs backscatter values (down) for a measurement point over the period Oct. 2008 – Oct. 2009..... 39*

*Figure 36 - Snow-depth vs backscatter values at Ku-band for the whole dataset. ..... 39*

*Figure 37 - Snow-depth vs backscatter values at S-band for the whole dataset. ..... 40*

*Figure 38 - Snow-depth vs backscatter values at S-band with std of each bin ..... 40*

# Table of Table

*Table 1 - NE Atlantic open ocean dataset ..... 13*

*Table 2 - Bay of Singapore open ocean dataset ..... 13*

*Table 3 - Adriatic Sea open ocean dataset ..... 14*

*Table 4 - NE Atlantic coastal ocean dataset ..... 19*

*Table 5 - Adriatic Sea coastal ocean dataset ..... 19*

*Table 6 - Svalbard polar ocean dataset..... 23*

*Table 7 - Track polar ocean dataset..... 23*

*Table 8 - River and lake level products..... 27*

*Table 9 - LOTUS test areas for Surface Soil Moisture derivation from Cryosat2 data ..... 29*

*Table 10 - Content of CSME Dataset Header 1..... 36*

*Table 11 - Content of CSME Dataset Header 2..... 36*

*Table 12 - Content of CSME surface Soil Moisture Dataset..... 37*

## 1. Abstract

The objective of this document is to present the results from the LOTUS project to the Copernicus Ocean and Land Services, together with recommendations. Several improvements beyond the state of the art were done during this project, especially on L1BS/L2 pre-processing and L2 processing algorithms. New L2 products were generated as prototype products. Assessment and assimilation in models of those datasets provided with interesting results for ocean and land applications. This document will then describe all results from the project to Copernicus services. Experimental products at higher levels also showed possible improvement for Copernicus datasets. Recommendations to Copernicus services will represent the main outputs of the current document.

# 2. Copernicus Marine Service

## 2.1. Major improvements

### 2.1.1. Open Ocean

#### *2.1.1.1. Major improvements using SAR altimetry*

The Sentinel-3 mission with its SAR-mode altimeter, SRAL, contains new features and capabilities which differ from the conventional radar altimeter. It uses a synthetic aperture processing for increasing the spatial resolution of the measurements along the satellite track direction (from tens of km to ~300 meters in width), and a multilook processing for increasing the effective number of looks in a stack (higher than the usual ~90 independent pulses averaged in LRM at 20-Hz) and thus improving the precision (lower noise) of the measurements. Thanks to those performance enhancements, SAR-mode altimeter data is able to improve recovery of short spatial scale phenomena over ocean (small eddies and fronts, internal waves and tides, as well as natural and man-made slicks, rain cells, or small-scale wind bursts and convective cells in an unstable atmospheric boundary layer, which would all cause rapid variations of the altimetric backscattered coefficient) and to resolve short-wavelength sea surface signals caused by sea-floor topography elements (sea- mounts/trenches) that cannot be detected when the footprint is too large, as for conventional altimetry.

With regard to the SAR-mode altimetry, three major features are observed: a) the reduction of the noise level (5.5 cm with respect to ~8 cm for LRM) even if it is not as high as expected due to the high inhomogeneity between Doppler beams in a stack, b) no correlated errors at short wavelengths (whereas a hump-shaped artefact is seen on the SLA power density spectrum from conventional LRM altimetry), and c) the ability of the SAR-mode processing to better capture small scale variations of the sea surface roughness, providing cleaner SLA observation.

In the frame of the LOTUS project, we have pursued work, in collaboration with the CNES French agency, on optimising the development of an ocean full numerical SAR model, to accurately reproduce the physics of the measurements including the instrument characteristics and the data processing. This method is considered to be more robust than analytical ones which are limited to simplified models and particularly inappropriate when faced with atypical observations (e.g., elliptical antenna pattern, off-nadir mispointing angles) and for unusual signal processing (e.g., distortions of the point target response, waveform aliasing) that could be readily handled in a numerical model but more difficult to put into equations. For the latter, such complexities necessarily involve analytical approximations that might lead to large and uncontrolled inaccuracies (systematic errors and geophysical dependent biases in the retrieval parameters), some of which may be corrected a posteriori while others do not. A numerical approach is free of these drawbacks.

#### 2.1.1.2. Assessment

A deep assessment done with Cryosat-2 data in open ocean and through different diagnoses has clearly demonstrated and quantified the improvement in altimetric performance obtained by using SAR-mode processing with its particular numerical retrieval approach compared to standard altimetry. We summarize below the most important and relevant evidence and findings from the Cal/Val process that illustrate the benefits of using this technology.

This validation exercise was carried out based on the use of two years of Cryosat-2 data and thanks to dedicated assessment methods and metrics for estimating their performance. In particular, the following diagnoses are considered:

- Analysis of the spectral content of the different geophysical retrieved parameters
- Assessment of the long wavelength errors based on comparison with co-localised PLRM data that are considered as our data sets reference (providing excellent agreement with Jason-2 parameters and seamless transition with LRM data)
- Assessment of residual errors linked to key parameters for the SAR processing that would suggest potential error in modelling

##### (i) Spectral analysis

One of the main relevant features is that the SAR-mode power spectra density does not show the spectral hump between 10 and 30 km (see Figure 1) while it is observed on the PLRM. This should yield better accurate observations to capture oceanic structures below 100 km.

It is also important to report the improved content for Sigma0 at scales below 100 km due to the 300 m footprint in the along track direction (the SAR-mode altimeter capturing smaller scale variations of the sea surface roughness are thus providing more energy as seen in Figure 2). This would suggest that the SAR processing better captures the sea surface roughness in the sigma0, and consequently providing a cleaner SLA observation.

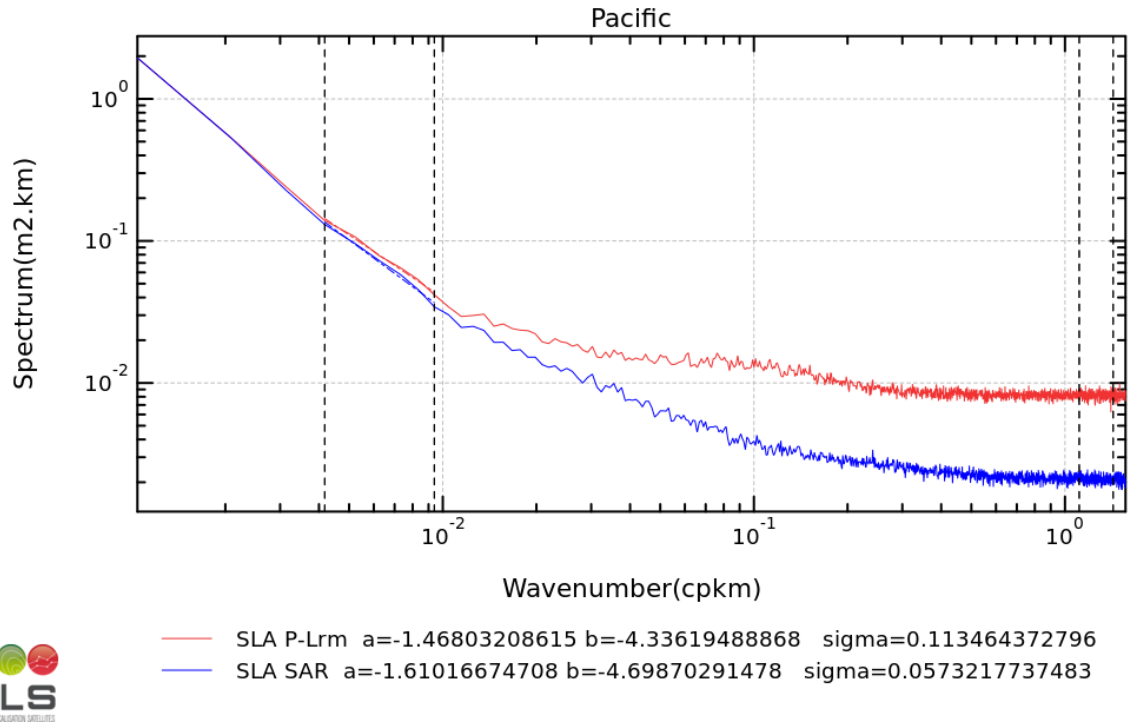


*Figure 1 - Power spectral density for SAR-mode and PLRM Sea Level Anomaly*

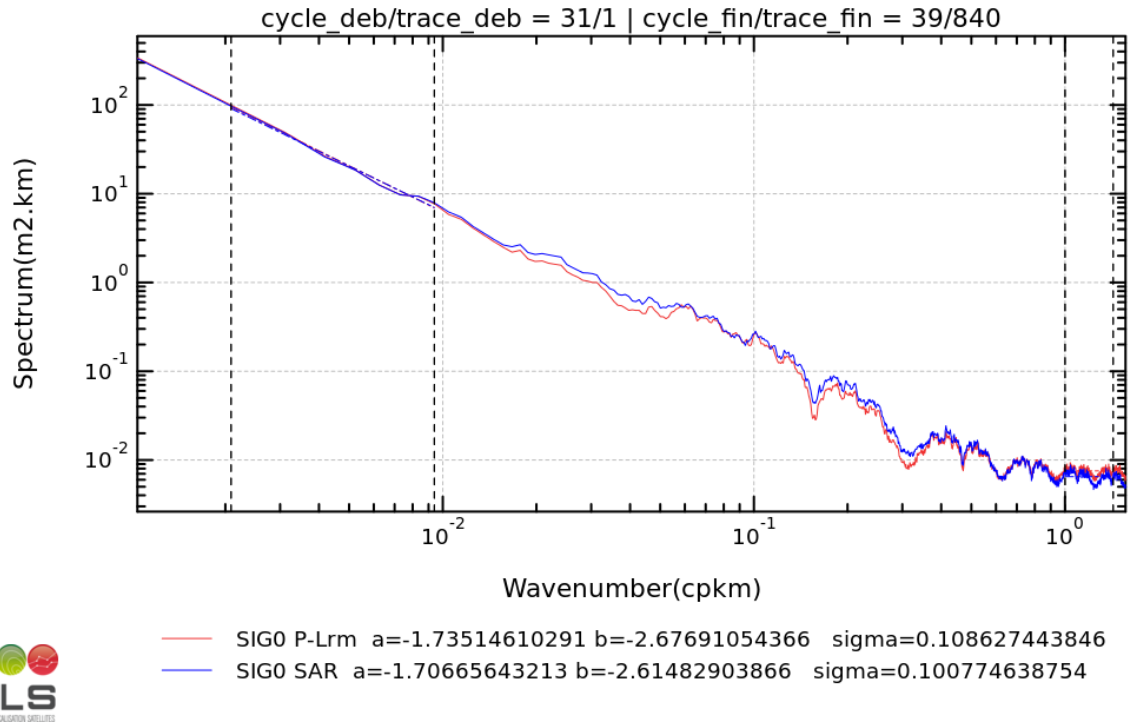


*Figure 2 - Power spectral density for SAR-mode and PLRM sigma-0*

### *(ii) Analysis of large scale biases compared to PLRM and dependencies*

The SLA shows neither residual errors correlated to mispointing, nor to radial velocity. Additionally, no dependency is observed for significant wave height higher than 2 m, which would suggest a similar SSB behaviour between LRM and SAR modes with the proposed processing. Discrepancies are however observed on low wave height (below 2 m), similarly for ascending and descending passes, and for which the accuracy of the estimates is in doubt due the particular steep shape of the leading edge of the SAR waveforms. This issue should be further confirmed with other SAR retrieval algorithms.

The Figure 4 shows that the absolute bias between SAR mode and PLRM is low and close to +3 cm as observed on the map of their difference (see in Figure 3).

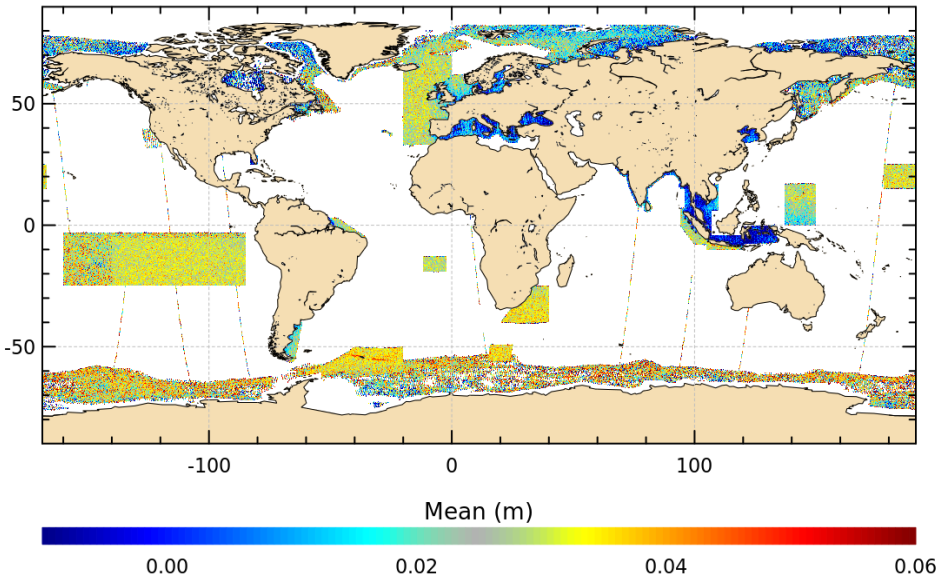


*Figure 3 - Maps of difference between PLRM and SAR Sea Level Anomaly*

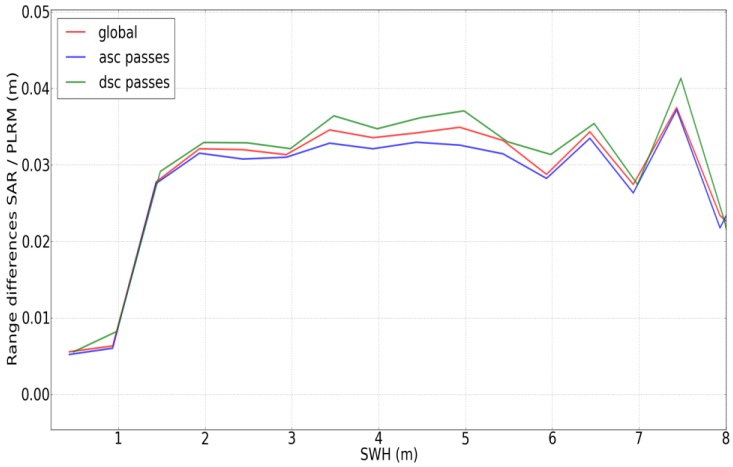


*Figure 4 - Difference between PLRM and SAR range as function of waves*

The SWH exhibits residual error correlated with SWH close to 2.5% SWH. This dependency does not vary in time, and bias on SWH is close to 15 cm at 2 m and around 20 cm for wave height higher than 4 m, which is good given the few areas in SAR mode and the complexity of the signals. Investigation is however on-going to understand this small discrepancy.

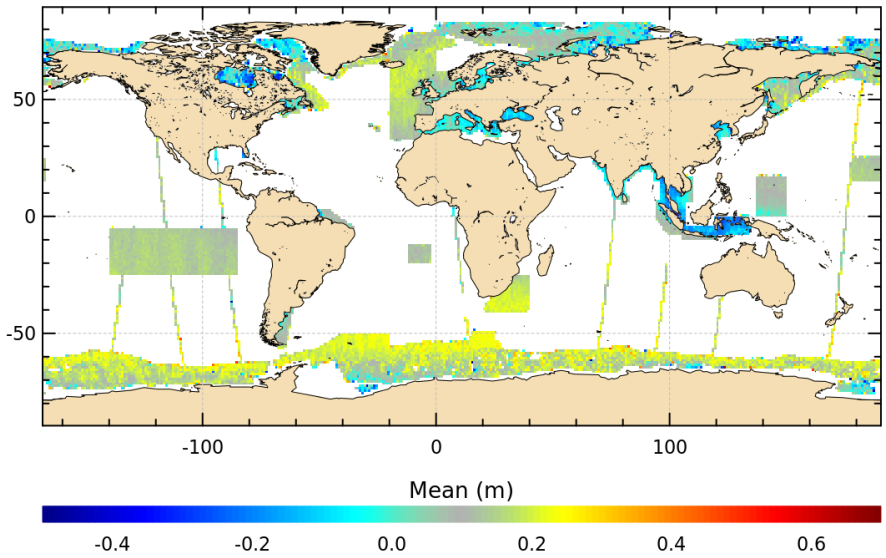


*Figure 5 - Maps of difference between PLRM and SAR significant wave height*

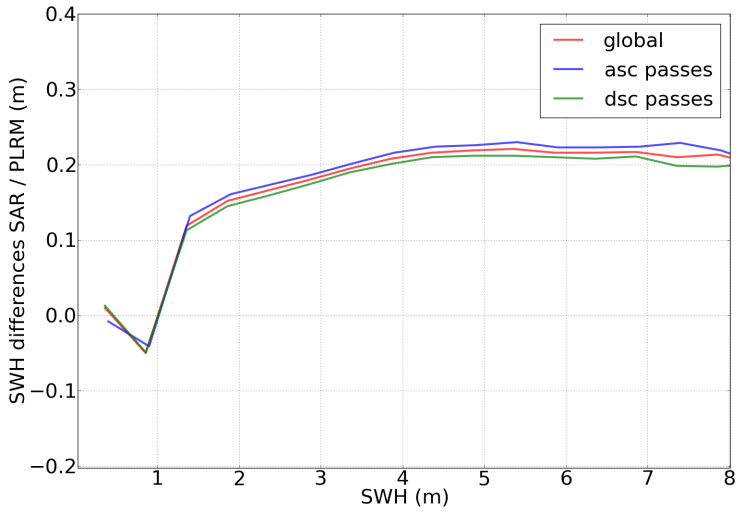


*Figure 6 - Difference between PLRM and SAR significant wave height as function of waves*

The map of the difference between SAR mode and PLRM sigma-0 is given in Figure 7. It exhibits an excellent agreement between both processings, showing variations of only 0.2 dB magnitudes, slightly correlated with respect to the along-track mispointing (pitch) as shown in Figure 8. This would suggest some inaccuracy in the pitch bias value computed between the star tracker boresight and the altimeter electromagnetic axis, impacting directly the estimation of the amplitude of the waveforms

since they are closely correlated. On the other hand, sigma-0 shows neither residual errors correlated to across-track mispointing (roll), nor to the significant wave height.

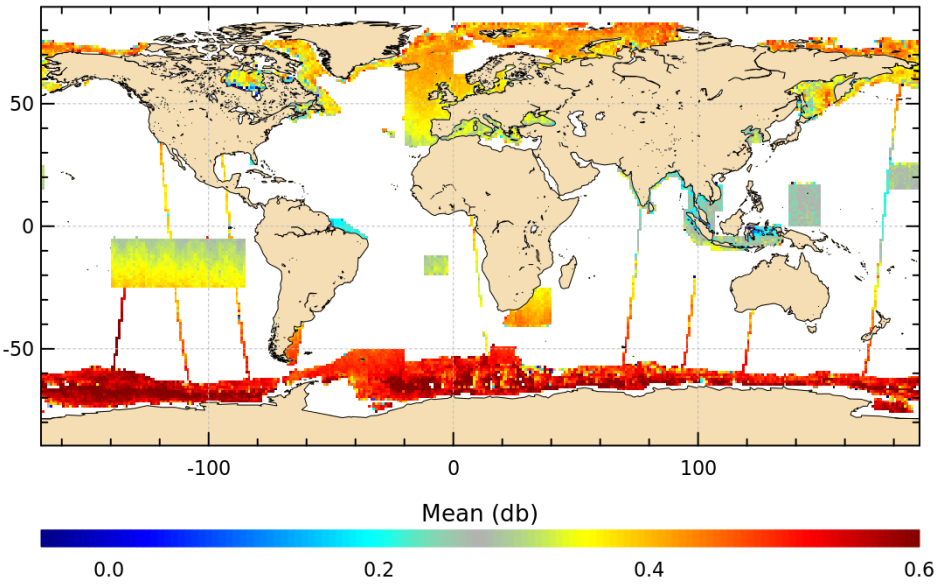


*Figure 7 - Maps of difference between PLRM and SAR sigma-0*

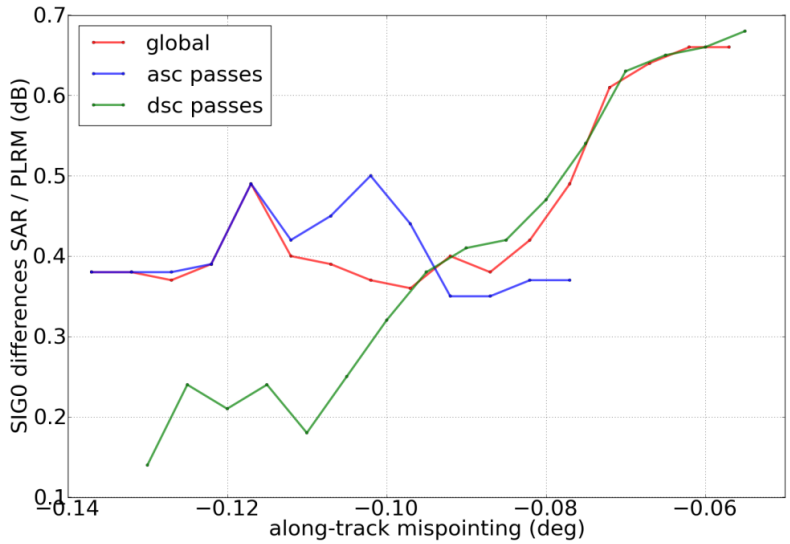


*Figure 8 - Difference between PLRM and SAR sigma-0 as function of along-track mispointing*

#### *2.1.1.3. Limitations*

The synthetic aperture processing creates Doppler bins as narrow as 300 meters in width, allowing to provide high-resolution (but also high-accuracy and precision) along track altimetric data and to better

resolve fine-scale features on the ocean surface. It clearly emerges that the improved along-track resolution from SAR-mode altimeter makes measurements potentially affected by sub-mesoscale structures (from 0.1 to 1 km) too, like swells, which are, on the contrary, averaged out and undetected in low-resolution mode observations. It is currently unknown how the retrieved sea surface height elevations and other surface parameters derived from the SAR-mode are impacted and at what accuracy these data are in the presence of directional ocean waves, especially those whose wavelengths are close to the SAR along track resolution. Further investigations have to be done to better address the sensitivity of the long-wavelength surface waves on SAR-mode measurements, and to determine a correction strategy accounting for the long swell in the SAR-mode retrieval. This issue is of high importance for the upcoming missions (Sentinel-3 and Sentinel-6 embarking a SAR-mode instrument).

#### *2.1.1.4. Products*

##### *(i) Level-2 datasets*

The OO_2_OCE Lotus product contains level-2 ocean geophysical parameters derived from Cryosat-2 SAR-mode data. This product also includes pseudo pulse-limited (PLRM) estimates derived from an incoherent processing of the same returning echoes, that aim at assessing the in-orbit performances of the SAR-mode data compared to well-known LRM-like data. Both retrievals are made at the same points along the ground tracks with thus identical time and location allowing for their direct comparison without the need to apply any environmental and geophysical corrections that may contribute to some potential differences and lead to unclear conclusions regarding the comparison between the different processing approaches.

Data are provided at two frequencies, 1 Hz and 20 Hz, and are sequentially split into NetCDF files, with one file per pass (one pass is a half-orbit, descending or ascending orbit). For each file, the datasets are organised in a standard structure that is close to the one used for Sentinel-3 products where 1 Hz and 20 Hz parameters are stored into separated variables. This way ensures ease of use for the user.

Three areas of interest have been selected for the prototype open ocean datasets: NE Atlantic, Bay of Singapore and Adriatic Sea.

*Table 1 - NE Atlantic open ocean dataset*

| Parameter | Value |
|---|---|
| **Geographical Coverage** | N.E. Atlantic<br>13W – 15E, 48N – 59N |
| **Temporal Coverage** | 1st May 2012 – 30th April 2014 |

*Table 2 - Bay of Singapore open ocean dataset*

| Parameter | Value |
|---|---|
| **Geographical Coverage** | Bay of Singapore<br>98E – 121E, 4S – 25N |
| **Temporal Coverage** | 1st May 2012 – 30th April 2014 |

*Table 3 - Adriatic Sea open ocean dataset*

| Parameter | Value |
|---|---|
| **Geographical Coverage** | Adriatic Sea<br>12E – 20E, 40N – 46N |
| **Temporal Coverage** | 1st May 2012 – 30th April 2014 |

### 2.1.2. Costal area

#### *2.1.2.1. Major improvements using SAR altimetry*

##### *(i) Along track direction*

The increasing interest of SAR mode altimetry, especially in coastal areas, is linked to the higher resolving measurement capability in the direction of the platform velocity, i.e. along-track direction. The improved resolution is a consequence of the delay-Doppler processing of the radar echoes. The along-track resolution reaches values typically around 250 to 300 meters (R. K. Raney, Resolution and Precision), which represents a remarkable improvement in comparison to the several kilometres currently achieved with conventional altimetry.

The shrinking of the radar footprint allows reducing the land contamination effect, which is the main limitation in the use of satellite altimetry for coastal areas. As a consequence of this, SSH, SWH, and WS measurements are expected to be provided at as close as several hundred meters from the shore. Various studies have already shown the capabilities of a delay-Doppler Altimeter to obtain useful radar echoes at a distance about 300 meters from the coast (e.g. Dinardo, Lucas, and Benveniste, 2011). As can be observed in Figure 9, waveform #1854, obtained from few hundred meters from the coast, was successfully retracked by the SAMOSA model.

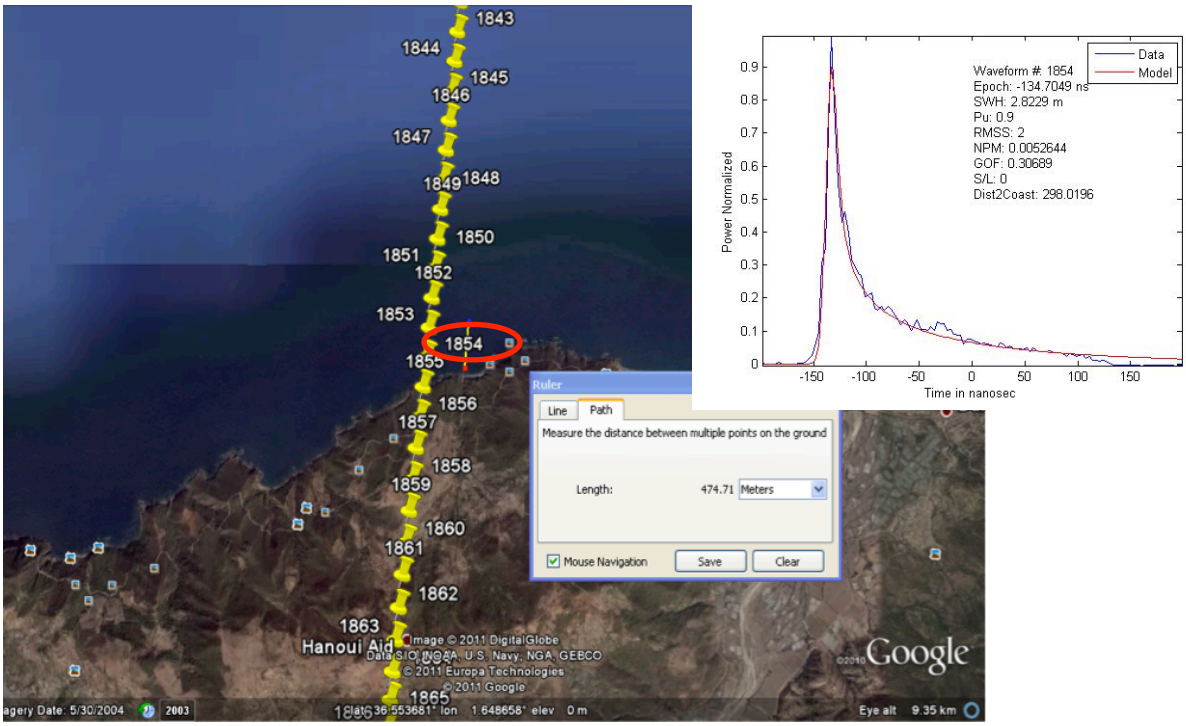


*Figure 9 - SAR Altimetry waveforms for satellite track perpendicular to the coast (along track)*

### *(ii) Across track direction*

As pointed out above, in a delay-Doppler altimeter the resolution improvement occurs only on the along-track direction, while the across-track direction remains pulse-limited. This implies that the DDA's response in coastal regions depends on the relative orientation between the coastline and the spacecraft orbital plane. The 250 m dimension prevails when the coastlines are perpendicular the flight direction, whereas the longer pulse-limited direction dominates when the altimeter is passing parallel to the shore. In, (e.g. Dinardo, Lucas, and Benveniste, 2011), the authors provided examples of CryoSat-2 SAR mode waveforms in this situation. As can be observed in Figure 10, despite the fact that the distance to the coast is almost 5 km, SAR waveform #56 is corrupted by a land effect in its tail, which prevents the use of this data for oceanographic applicatons.

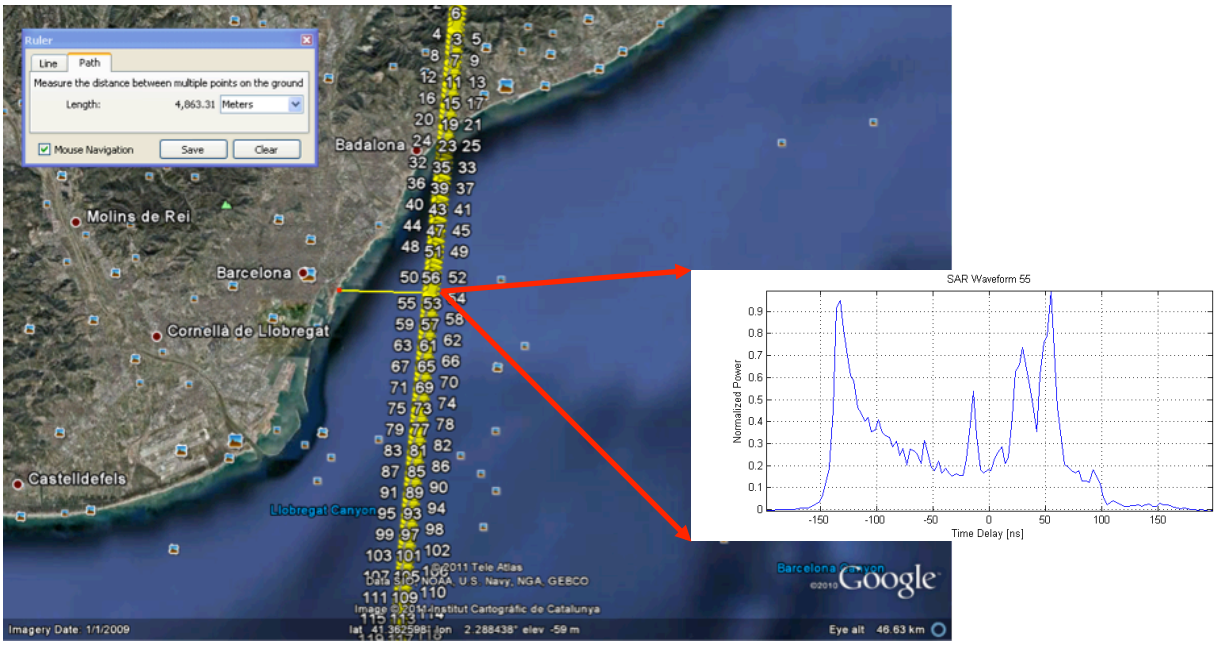


*Figure 10 - SAR Altimetry waveforms for satellite track parallel to the coast (across track)*

Within the LOTUS project we have developed an algorithm that process (pre-process) the waveform to obtain the correct estimated waveform close to the coast for a track parallel to the coastline. The algorithm disregard the range bins of the SAR waveform which are likely to be affected by land contamination. This is achieved by geo-locating the delay and Doppler pairs of the SAR Altimeter stack, i.e. the 2-dimensional array for the range cell migrated Doppler looks aligned with respect to the nadir position. The SAR waveform retracker is then fed with this information and neglects the range bins subjected to land contamination from the geophysical parameter estimation process.

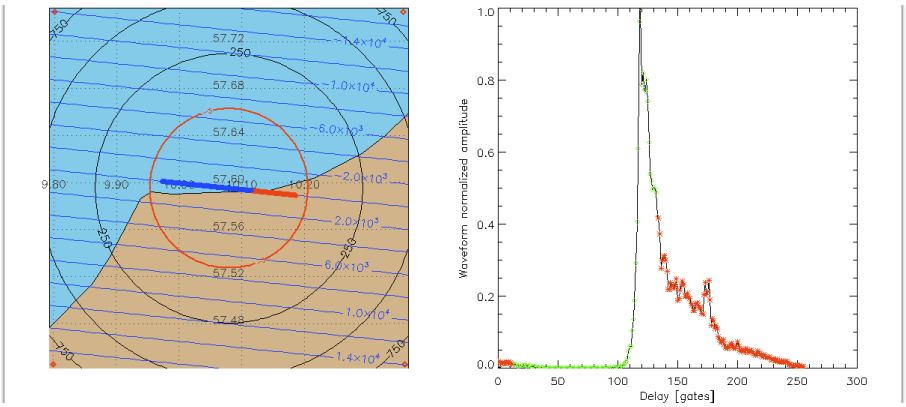


*Figure 11 - SAR Altimetry waveforms for satellite track contaminated by land in the across track direction. Location of the track and the studied beam (left). Waveform pre-processed (red point rejected) to be ingested into the SAR waveform retracker (right).*

#### 2.1.2.2. Assessment

The method provides with good results at 20 Hz. The comparison between pre-processing + SAMOSA and the results obtained using the CPP retracker shows a good correspondance between both methods.

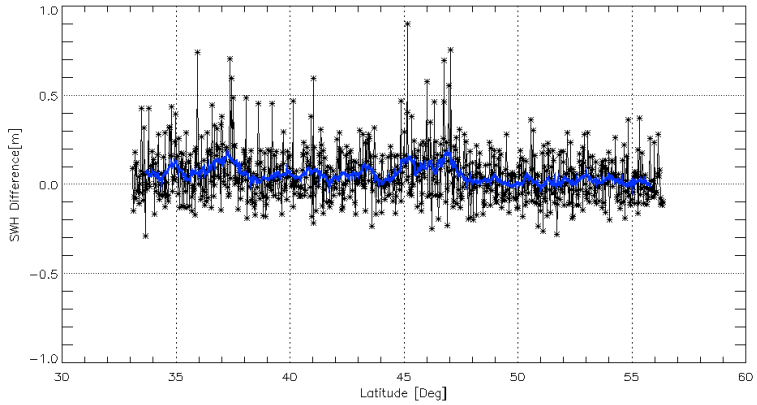


*Figure 12 - Coastal area pre-processing (+ SAMOSA retracker) assessment using as reference CPP retracking solutions. SWH difference along a specific track*

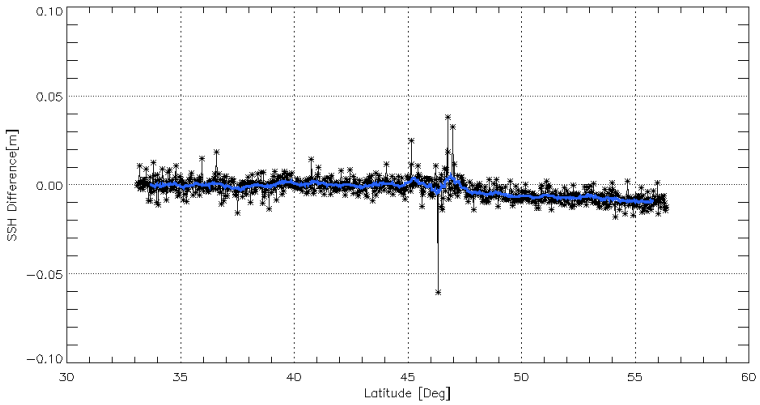


*Figure 13 - Coastal area pre-processing (+ SAMOSA retracker) assessment using as reference CPP retracking solutions. SSH difference along a specific track*

#### 2.1.2.1. Limitations

Such method provides interesting results regarding reference datasets. However, it constitutes in a first approach that needs improvement to be robust to every kind of coastal perturbations. The method only takes into account across track perturbations. The following study establishes a first trends about the results in comparison with in-situ measurements.

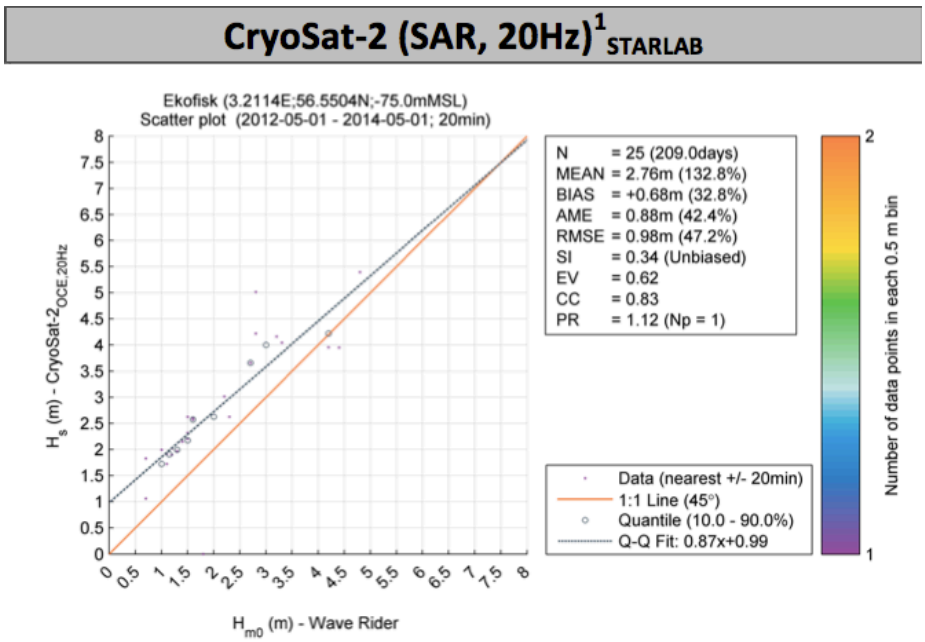


*Figure 14 - Coastal retracker vs. in-situ SWH (Hs) at Ekofisk, (Central north sea station)*

The method suffer some limitations, in particular due to land contamination in the along track direction, or to shallow water. Such situation produce perturbed waveform that can not be process by the coastal retracker (pre-processing); the digital elevation model does not enconter land (positive altitudes) in the accross track direction.

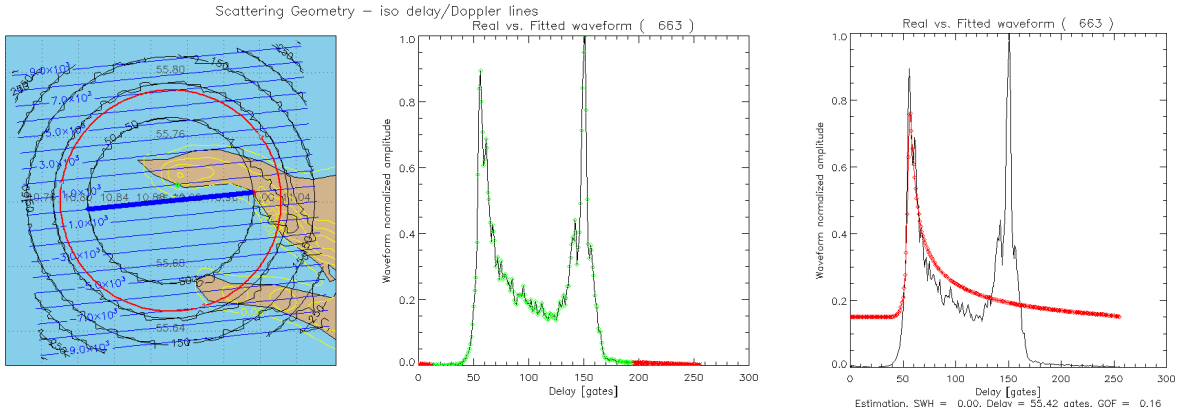


*Figure 15 - Waveform retracking through the coastal retracker. Waveform perturbed by the presence of land in the along-track direction.*

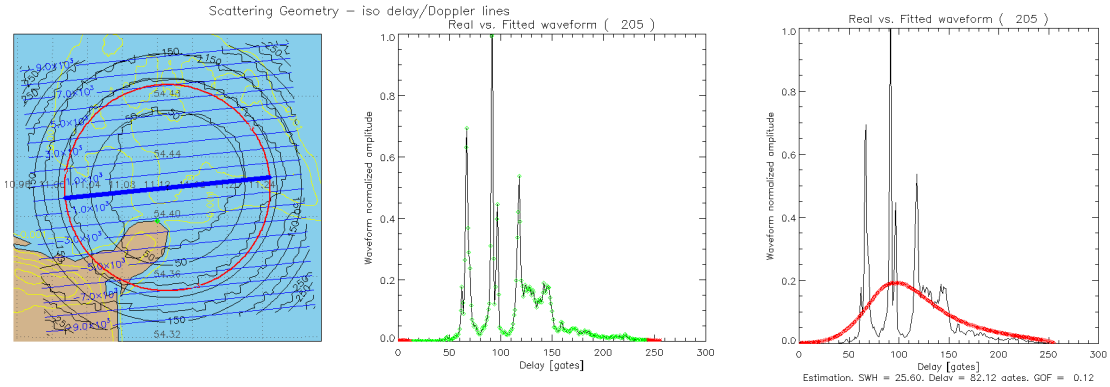


*Figure 16 - Waveform retracking through the coastal retracker. Waveform perturbed by the presence of shallow water.*

#### 2.1.2.2. Products

This data product contains 20Hz Coastal Sea parameters over selected areas. The data is stored in a NetCDF file using Climate Forecast (CF) convention. Data has been processed according to the algorithm, which is described in 0.

Two areas have been selected for the prototype coastal area datasets: NE Atlantic and Adriatic Sea.

*Table 4 - NE Atlantic coastal ocean dataset*

| Parameter | Value |
|---|---|
| **Geographical Coverage** | N.E. Atlantic + North Sea<br>15W – 17E, 46N – 61N |
| **Temporal Coverage** | 1st May 2012 – 30th April 2013 |

*Table 5 - Adriatic Sea coastal ocean dataset*

| Parameter | Value |
|---|---|
| **Geographical Coverage** | Adriatic Sea<br>10E – 22E, 38N – 48N |
| **Temporal Coverage** | 1st May 2012 – 30th April 2013 |

### 2.1.3. Polar Ocean

#### *2.1.3.1. Major improvements using SAR altimetry*

The Sentinel-3 mission with its SAR-mode altimeter, SRAL, contains new features and capabilities which differ from the conventional radar altimeter. The prime advantage is that the delay processing reduces the footprint considerably (from more than 100 km2 to less than 10 km2). Hence the chance of retrieving non-ice contaminated footprint is far greater than for conventional LRM altimetry.

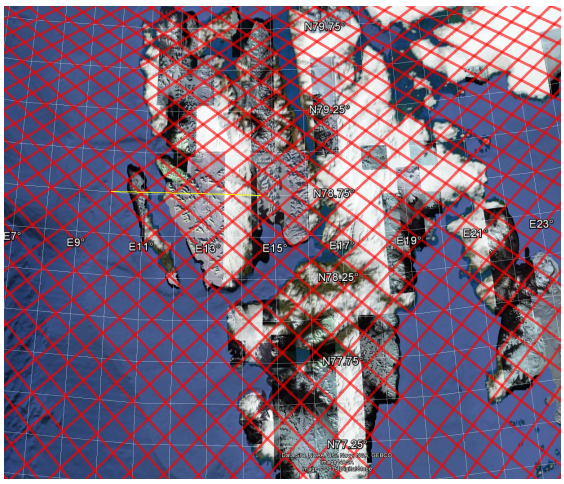


*Figure 17 - The Sentinel-3A tracks in the Polar Ocean. Here around Svalbard. The yellow line at 78.75 is 100 km long and demonstrate that the across track distance at this latitude is around 20 km.*

The use of a synthetic aperture processing for increasing the spatial resolution of the measurements along the satellite track direction (from tens of km to ~300 meters in width), and a multilook processing for increasing the effective number of looks in a stack (higher than the usual ~90 independent pulses averaged in LRM at 20-Hz) will further improve the precision (lower noise) of the measurements in the Polar Ocean compared with conventional altimetry from ERS-1/ERS-2/ENVISAT.

In the Arctic Ocean less than 20% of the radar pulses are actually returned from the ocean surface in the leads but instead from sea ice floes, ice ridges and other ice surfaces. For the Sentinel-3 SAR the pulse peakiness (PP) and stack standard deviation (SSD) is used to classify the radar returns from leads and non-leads, see Figure 18. Typical values for classified leads are SSD<3 and PP>0.26 and ocean when SSD>40 and PP<0.1. These numbers reflect that lead waveforms are very narrow peaked. Consequently these are frequently very well retracked using a threshold retracker using a stabilized maximal threshold in which only the sea surface height is considered. This is under the assumption that for leads the significant waveheight is zero and the wind speed is hard to detect.

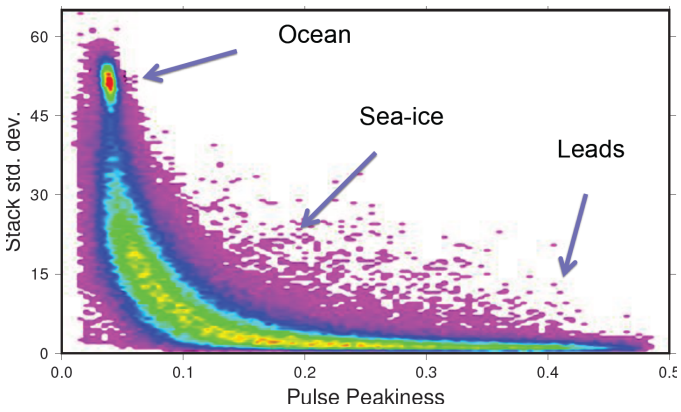


*Figure 18 - Classification in the Arctic Ocean for Sentinel-3*

#### 2.1.3.2. Assessment

A procedure to detect areas with open water or newly refrozen leads in aerial photos has been developed and applied on data from three IceBridge in 2012 and 2013 to validate the classification of the radar returns. For the IceBridge underflights 80% of leads above 500 m2 can be classified (Se example in Figure 23. Consequently this classification were compared with the classification by pulse peakiness and stack standard Deviation (SSD) as described above for the simultaneous Cryosat-2 track and the comparison is shown in Figure 23. with the area of lead from IceBridge shown in Red and the Cryosat-2 detection shown in Blue. When comparing the IceBridge laser height with collocated retracked CryoSat-2 the average difference is 0 cm, but only 34 point was available for the comparison.

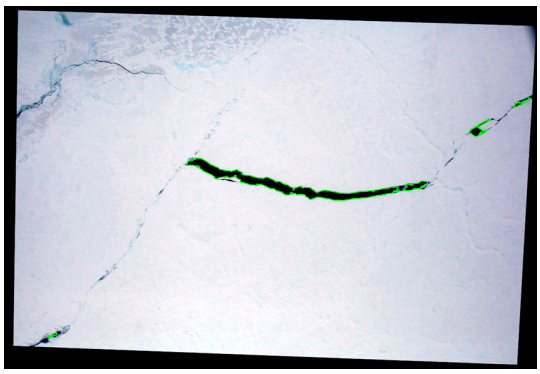

*Figure 19 - Example of lead detection in area photos from IceBridge co-located Cryosat-2 tracks in the Arctic Ocean in 3013.*

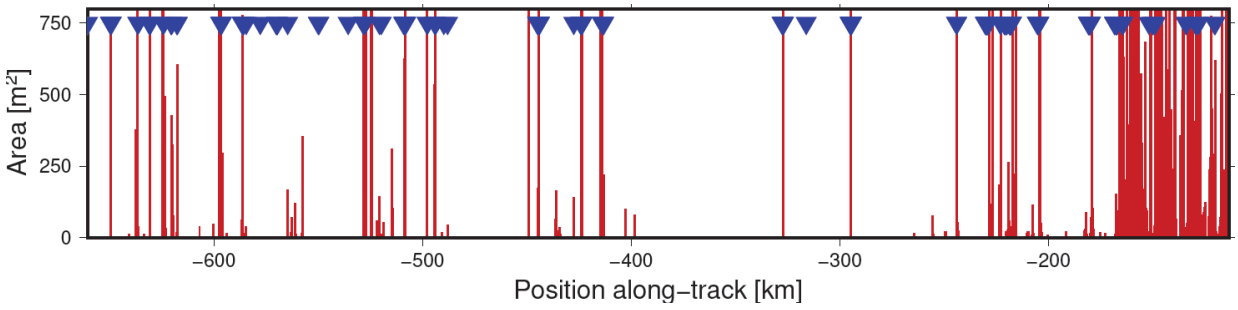

*Figure 20 - A total of 34 leads detected by Cryosat-2 (blue) and by the size in the co-located IceBridge area photos.*

An assessment of the derived height in the test region surrounding Svalbard was done to validate the retracker. Unfortunately, we were only able to use the monthly sea level time series from the Permanent Service for Mean Sea Level in a comparison with the LOTUS project dataset. The daily timeseries and the annual comaparison with the Svalbard tide gauge is shown inFigure 23.

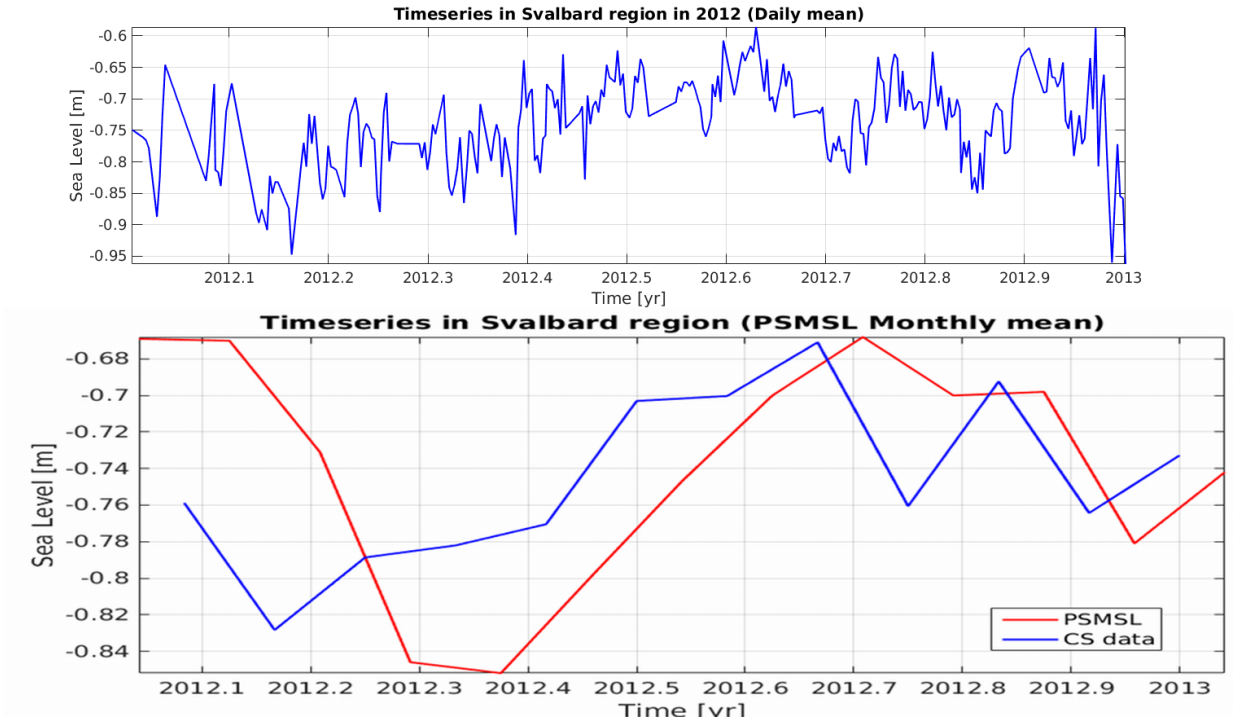


*Figure 21 - The LOTUS Cryosat-2 daily time series in the Svalbard region and the comparison with monthly sea level data from PSMSL.*

### 2.1.3.3. Limitations

Prior to SAR altimetry it was virtually impossible to use satellite altimetry in large parts interior of the Arctic Ocean which was seasonaly ice-covered, but with Cryosat-2 and Sentinel-3 it will be possible to determine accurate sea level changes in the Arctic Ocean up to the inclination of the Sentinel-3 satellite (81.5 N). Above this latitude it is will still not be possible to study sea level variations in the Arctic Ocean. In all investigations so far we have seen considerably longwave errors in the Cryosat-2 and these were also presented at the recent AGU meeting. The origin of these long wavelength errors are still not fully understood (can be orbit related errors or mispointing errors) and we do not know if these are specific to Cryosat-2 or will be an issue for Sentinel-3 as well, but they sure requires further investigation in order to achieve the full potential of the Sentinel-3 data for the Polar Ocean.

#### 2.1.3.4. Products

This data product contains 20Hz Polar Ocean parameters over selected areas. The data is stored in an ascii files with names corresponding to the original L1 data files delivered by ESA. Data has been processed according to the algorithm, which is described in 0 for the Polar Ocean.

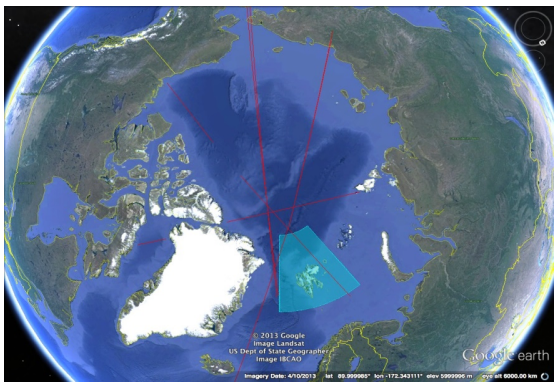


*Figure 22 - The Svalbard polar ocean region (light blue) and the track polar ocean dataset (red)*

*Table 6 - Svalbard polar ocean dataset*

| Parameter | Value |
|---|---|
| **Geographical Coverage** | Svalbard<br>0E – 40E, 75N – 85N |
| **Temporal Coverage** | 2012 |

*Table 7 - Track polar ocean dataset*

| Parameter | Value |
|---|---|
| **Geographical Coverage** | Over North pole |
| **Temporal Coverage** | 2011-2013 |

## 2.2. Recommendations

### 2.2.1. Open ocean

Given the clear benefits of using SAR-mode data and its potential interest for the development of new marine applications, the altimetry community acknowledges the need to go a step further in operating this mode over 100% sea surfaces (as it is planned for Sentinel-3 mission and the next Sentinel-6). In

order to deliver such operational services and provide useful SAR-mode products for the end-users, a structured process has to be established which consists in:

- developing a level-2P production system (including editing, filtering, geophysical correction, orbit error correction and subsampling) to prepare the generation of the level-3 along-track products for the Copernicus Marine Service (CMS)
- generating level-3 products for data assimilation systems of the CMS
- generating level-4 products for various applications (currents, Search& REscue, climate, …)

### 2.2.2. Coastal area

SAR altimeter by itself can significantly improve the estimation of the ocean parameters (SSH, SWH…) in the coastal areas. The along-track resolution reaches values typically around 250 to 300 meters (R. K. Raney, Resolution and Precision), which represents a remarkable improvement in comparison to the several kilometres currently achieved with conventional altimetry.

The coastal processing of SAR waveform developed in the LOTUS project shows that SAR waveform retracking can also be improved in the across track direction using a pre-processing step that clean the waveforms from land contamination. However, a specific attention should be taken to additional situations such the presence of land in the along track direction, or the presence of shallow water to fully provide an operational algorithm that could be introduced as coastal products, or to extend SAR altimeter products using Cryosat-2 and, in the future, Sentinel-3 data.

### 2.2.3. Polar ocean

SAR altimetry is a huge step forward for Polar Ocean sea level research. This is particularly due to the enhancement in along track resolution (300 meters), the smaller footprint in the SAR processing, and the improved capabilities using the SAR stack information in determining the leads in the ocean and to discriminate lead and contaminated returns. Prior to SAR altimetry it was virtually impossible to use satellite altimetry in large parts interior of the Arctic Ocean which was seasonaly ice-covered, but with Cryosat-2 and Sentinel-3 it will be possible to determine accurate sea level changes in the Arctic Ocean up to the inclination of the Sentinel-3 satellite (81.5 N). Above this latitude it will still not be possible to study sea level variations in the Arctic Ocean. For the Polar Ocean we recommend that procedures similar to the procedure suggested above for the open ocean is set in place and combined with the screening of the data for lead and ocean described above.

# 3. Copernicus Land Service

## 3.1. Major improvements

### 3.1.1. River and lakes

#### *3.1.1.1. Major improvements using SAR altimetry*

Radar reflections from inland water bodies show a large diversity in the shape of the waveform. Figure 23 shows examples of typical waveforms. Very still standing water is an efficient reflector and therefore produces a specular waveform, while a more rough water surface produces an ocean like waveform (second panel in Figure 1). Waveforms from inland water are typically also contaminated with signals that originate from the surrounding land; hence these waveforms will often contain multiple peaks. It is therefore a great challenge to derive the actual water level from such waveforms.

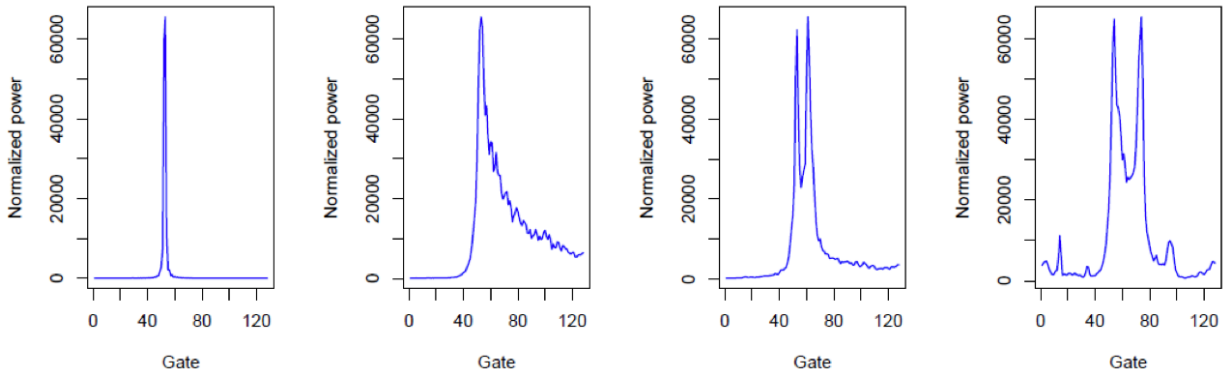


*Figure 23 - Examples of SAR echoes related to inland water bodies*

A specific process has been developed to select the correct waveform and estimate the corresponding water level. For each waveform a subwaveform is extracted based on start and stop thresholds. These thresholds are found from the standard deviation of the power differences in consecutive bins (Jain et al., 2015). Once the subwaveform is extracted, the retracking bin is found by applying a threshold retracker on the subwaveform. The retracker is referred to at the Narrow primary peak threshold retracker (NPPTR).

In a post-processing procedure the MODIS mask is used to identify measurements over a given in-land water body. For each track that contains more than 5 measurements a robust mean water level is estimated in addition to the retracked water levels. The algorithm flow charts are presented hereafter.

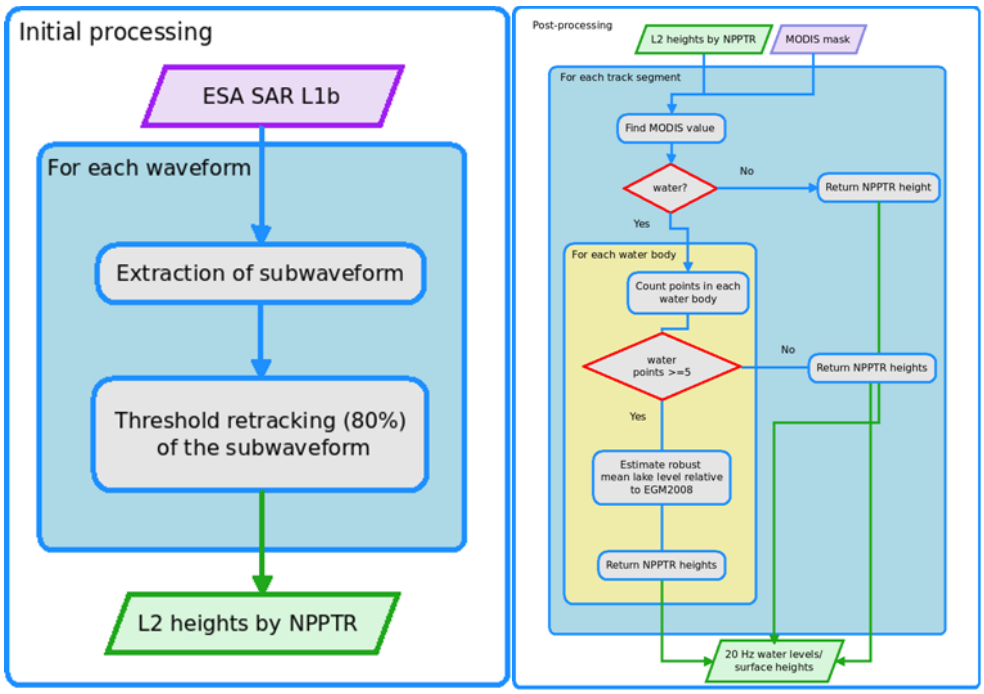


*Figure 24 - (Left) Flow chart describing the steps in SAR retracking procedure. (Right) Flow chart describing the steps in the post-processing*

#### 3.1.1.2. Assessment

##### (i) Danish lakes

For the Danish area we have extracted data over 22 lakes for validation. For Arresø, Mossø, and Skanderborg sø we have estimated the precision. We find that the precision of the water levels that are based on CryoSat-2 measurement in SAR mode are just a few centimetres for these lakes. For EnviSat the precision is approximately 20 cm. Hence, compared to EnviSat, the results that we have obtained with CryoSat-2 for these small lakes are a major improvement.

We have further estimated the average lake heights for 22 selected lakes in Denmark with a surface area ranging between 1 and 40 $km^2$. For ten lakes we have independent water level data based on Lidar data or officially given water levels. In general our CryoSat-2 based heights agree within 18 to 37 cm, except for Fårup sø and Gyrstinge sø. In most cases the Saral/Altika based heights are off by several meters, which indicate that there is something wrong with these data.

For Arresø we have in situ data for 2013, hence we have the possibility to validate the temporal height variations. For the CryoSat-2 based water levels we find an agreement within 1 to 4 cm. The amplitude of the temporal signal is approximately 20-25 cm according to the in situ data. This amplitude would not be possible to measure accurately with EnviSat, since its precision is at the same magnitude for this lake. Hence, this proves that CryoSat-2 in SAR mode opens new possibilities in terms of how accurately we can measure.

#### *(ii) Amazon river*

CryoSat-2 water levels of a river are much more challenging to validate, due to the drifting track pattern. For segment of the Amazon River used in this validation study, the terrain can be approximated with a constant slope. Since no in situ data is available we validate our CryoSat-2 water levels with satellite radar altimetry data from Saral/Altika. However, the problem with this is that the Saral/Altika data also contain erroneous observations. Hence, we can only do a relative validation.

When comparing the precision of the along track mean value, we find that the precision of CryoSat-2 is better. We have further estimated the measurement error of the individual observation and again we find that the CryoSat-2 water levels have the lowest error. Hence we can conclude that we obtain more accurate results with CryoSat-2 in SAR mode compared to Saral/Altika.

#### *(iii) Chao Phraya, Thailand*

The Chao Phraya River system in Thailand is a complicated system consisting of several different branches. The rivers are very narrow and primarily oriented in the North-South direction, which makes it very challenging to measure the water level with radar satellite altimetry. Due to the complexity of the terrain and the drifting track pattern is has not been possible to estimate a quality measure for this test data set and it should therefore be used with caution.

##### *3.1.1.1. Products*

This data product is available in netcdf format and contains 20 Hz River and lake levels relative to the reference ellipsoid WGS84. This product also contains an along track mean value for each inland water crossing, which can be used directly to generate time series.

The individual columns in product RL_2_LAN are explained in Table 8.

*Table 8 - River and lake level products*

| Short Name | Long Name | Unit | Description |
|---|---|---|---|
| **Point characteristics** | | | |
| time | time | second | seconds since 2000-01-01 00:00:00.0 |
| lat | latitude | degrees_north | Latitude of the point |
| lon | longitude | degrees_east | Longitude of the point |
| **Inland water/Land parameters** | | | |
| wl_se | Water level/ Surface elevation | m | Water levels or surface elevations relative to WGS84, based on the Narrow Primary Peak Threshold retracker (NPPTR). The following corrections are included: model ionosphere, model dry troposphere, modelled wet troposphere, solid earth tide, ocean loading tide, geocentric pole tide. |
| mwl | Mean water level | m | Robust estimate of the along-track mean water level |

| Short Name | Long Name | Unit | Description |
|---|---|---|---|
| | | | relative to EGM2008. This value is only returned if a water body contains 5 or more measurements otherwise the value 99999 is returned |
| **Atmospheric/Land corrections** | | | |
| Iono_corr_gim | GIM ionospheric correction | m | An ionospheric correction must be added (negative value) to the instrument range to correct this range measurement for ionospheric range delays of the radar pulse |
| tropo_dry_corr_mode<br>l | Model dry tropospheric correction | m | Computed at the altimeter time-tag from the interpolation of 2 meteorological fields that surround the altimeter time-tag. A dry tropospheric correction must be added (negative value) to the instrument range to correct this range measurement for dry tropospheric range delays of the radar pulse |
| tropo_wet_corr_model | Model wet tropospheric correction | m | Computed at the altimeter time-tag from the interpolation of 2 meteorological fields that surround the altimeter time-tag. A wet tropospheric correction must be added (negative value) to the instrument range to correct this range measurement for wet tropospheric range delays of the radar pulse |
| solid_earth_tide | Solid earth tide height | m | Calculated using Cartwright and Tayler tables and consisting of the second and third degree constituents. The permanent tide (zero frequency) is not included |
| pole_tide | Geocentric pole tide height | m | Deformation of the Earth induced by polar motion |
| ocean_load_tide | Ocean loading tide | m | Deformation of the Earth due to the weight of the overlying ocean tide. The FES2004 loading tide model is used for this correction |
| geiod | Geoid | m | EGM2008 |
| **Additional information** | | | |
| modis | MODIS mask value | | Value that indicates the underlying surface type; water =1, land=0 |

### 3.1.2. Soil moisture

#### *3.1.2.1. Major improvements using SAR altimetry*

Determining soil moisture from satellite radar altimetry is a relatively new application (e.g. Berry & Carter, 2010; 2011). This method is critically dependant on the development of detailed DRy Earth ModelS (DREAMS), which encapsulate the complex and rapid spatial changes in surface characteristics.

### *(i) DREAM Casting*

In order to retrieve soil surface moisture data from satellite radar altimetry, a detailed model of the surface backscatter response must be constructed. For the first application of this method in the ESA SMALT project (Berry et al., 2012; ESA SMALT, 2014) models were constructed using ERS1 satellite altimeter recalculated backscatter, cross-calibrated with additional satellite altimeter data. Analysis of repeat arc data was then made to identify and screen out remaining paleo-hydrology signatures in the DREAMS. From this, soil surface moisture estimates were made (ibid). However, the long repeat cycle of Cryosat2 precluded this approach and required a complete re-casting and rebuild of the DREAMs.

Accordingly, multi-mission altimeter backscatter was fused with ground truth information including terrain and surface component data. Additional waveform analysis and screening tests were introduced. The enhancements of this extensive rebuild were demonstrated when Jason2 data were used to calculate soil moisture successfully over all three test desert DREAMs (Berry & Balmbra, 2015a; 2015b). The SMALT project was only able to generate data from Jason2 over the Tenere desert (ESA SMALT, 2014), and these data were found to be erroneous.

The three defined primary test regions for soil surface moisture production are listed in Table 9. The Latitude/Longitude boundary coordinates form the primary geographically based selection of data over the regions of interest.

*Table 9 - LOTUS test areas for Surface Soil Moisture derivation from Cryosat2 data*

| Desert | Lower Longitude Bound (Degrees) | Lower Latitude Bound (Degrees) | Higher Longitude Bound (Degrees) | Higher Latitude Bound (Degrees) |
|---|---|---|---|---|
| Simpson | 135.0 E | 28.0 S | 139.0 E | 24.0 S |
| Tenere | 9.0 E | 15.0 N | 16.0 E | 21.0 N |
| Kalahari | 18.0 E | 27.0 S | 28.0 E | 17.0 S |

For all deserts, all SMALT masking was retained. Thus any area on any DREAM excluded from use in SMALT was excluded here. The rationale for this initial decision was that the additional masking was present because of the presence of inland water, paleo-hydrology features or large-scale roughness changes (e.g. mountains). The effect of these features on the DREAM accuracy had been quantified using repeat arc data from ERS2 (Berry et al., 2012).

The Simpson desert was chosen because it has no surface drainage, and thus no paleo-hydrology signatures. Its surface composition is also uniform. Whilst the dunefield characteristics change very significantly over this desert, their spatial variation is coherent, and the dune heights are very consistent within each part of the desert. Thus the large-scale roughness changes slowly and the small-scale roughness variation was modelled using results from an extensive field survey (Berry & Carter, 2010; 2011). The Simpson desert Dry Earth Model (DREAM), re-formed and re-masked for use with Cryosat2 data, is shown in Figure 11.

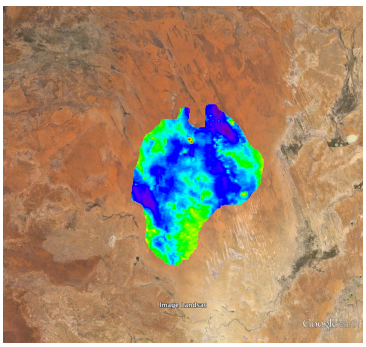

*Figure 25 - Simpson desert DREAM for CryoSat-2*

Because the Simpson desert DREAM is generated from such well-modelled terrain, this is the primary land backscatter calibration site for soil moisture determination, and was thus included. However, it receives occasional aperiodic rainfall and thus validating Simpson desert Cryosat2 derived soil moisture is critically dependent on the chance of precipitation during the validation period. This problem was illustrated when the Jason2 validation soil moisture dataset (from the one Jason2 track that crosses the Simpson DREAM) was graphed (Figure 12). The data are shown extending beyond the end of the validation year (2013) in order to include a significant soil moisture measurement following a rain event in 2014.

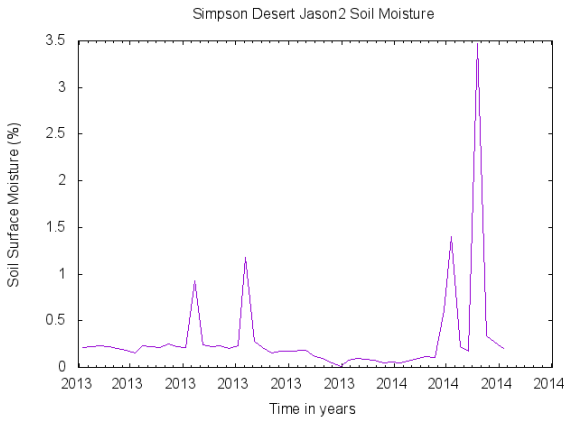


*Figure 26 - Simpson desert CSME validation soil moisture from Jason2 using enhanced DREAM*

The characteristics of different parts of the Sahara desert vary widely, and so one sub-desert region, the Tenere, was chosen, principally because prior work with ERS2 soil moisture had shown a small but clear annual signature across the region. This indicated that some signal might be detectable with Cryosat2, even though the long repeat period precluded repeat arc analysis, a critical component of all prior work on altimeter derived soil moisture (Bramer & Berry, 2010: Berry & Carter, 2011: Berry et al., 2012). This test region therefore represented the most challenging region with only a small soil moisture annual signature.

The re-calculated Tenere desert DREAM for Cryosat2 is illustrated in Fig.19, with the Jason2 track locations. Note that further dynamic masking is performed on data over this model in addition to the masking within the DREAM (DREAM masking is shown as transparent zones within the model). Jason2 data were also used with the enhanced DREAM to generate a validation timeseries (Figure 13). Two primary tracks are shown that cross different parts of the desert (Berry & Balmbra, 2015a; 2015b). Very clear annual signatures are seen, varying in magnitude according to the track location within the desert (ibid). Data were again generated for a slightly longer period than the validation year in order to discern the annual variation more clearly.

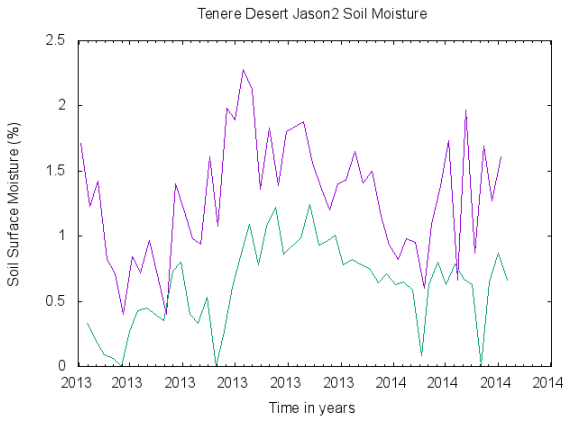


*Figure 27 - Tenere desert CSME validation dataset from Jason2 using enhanced DREAM*

The third test region chosen was the Kalahari desert. This is a challenging region in terms of building a DREAM, but there is a significant annual variation in precipitation and thus this desert offered the best chance of detecting an annual signature in the Cryosat2 data. The Cryosat2 DREAM for the Kalahari desert is shown in Figure 14. For this desert, the masking used for the ESA SMALT project is retained, with additional dynamic masking utilized during data production for this desert. Note that part of the Eastern Kalahari desert has been excluded from this model, following the ESA SMALT masking protocols (ESA SMALT, 2014), due to the presence of the Okavango delta and its input rivers.

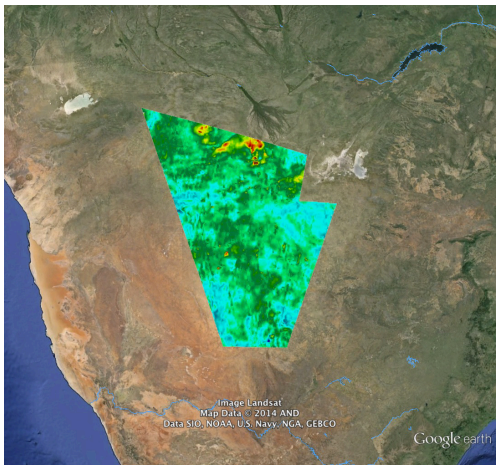


*Figure 28 - Kalahari desert DREAM for CryoSat-2*

For this desert, Jason2 data were again processed to form a validation dataset, using the enhanced DREAM developed for Cryosat2. Although the ESA SMALT project was not able to generate soil moisture products over the Kalahari desert (ibid), data were successfully created using the enhanced Kalahari Cryosat2 DREAM. Results from the two primary tracks used for validation are shown in Figure 15, again generating slightly more than the validation year in order to identify the annual signature clearly.

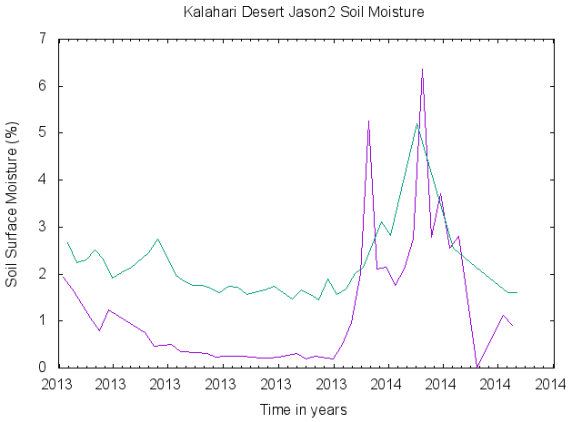


*Figure 29 - Kalahari desert CSME validation dataset from Jason2 using enhanced DREAM*

### (ii) SAR – LRM Comparison

Because all deserts were overflown by Cryosat2 in LRM mode, the product generation and testing have been on LRM data. An additional study was therefore carried out on the Gibson desert, where a single pass of SAR mode Cryosat2 data was acquired early in the mission. A result from this analysis is included here (Figure 16).

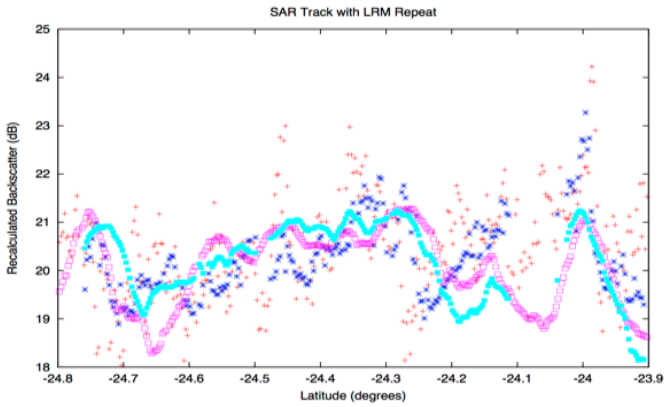


*Figure 30 - Cross-calibrated recalculated Cryosat2 SAR mode (red) and LRM (blue) backscatter with underlying DREAM pixels (SAR pink, LRM green)*

It is clear that the backscatter values from the single Gibson pass of data are in quite good agreement with the Gibson DREAM, especially considering that this DREAM has not yet been rebuilt using the

augmented Cryosat2 DREAM generation system. However, assessment of the SAR mode measurement precision and its potential improvement over LRM mode data must wait for Sentinel3.

The most significant enhancement during the LOTUS project has been the major improvement achieved in the quality of the DREAMS.

#### (iii) Processing Chain

An overview of the processing chain developed for Sentinel-3 Soil Moisture generation is given in Figure 31. More detail on the processing chains is given in the ATBD (Berry & Balmbra, 2014) and the LOTUS WP6 report.

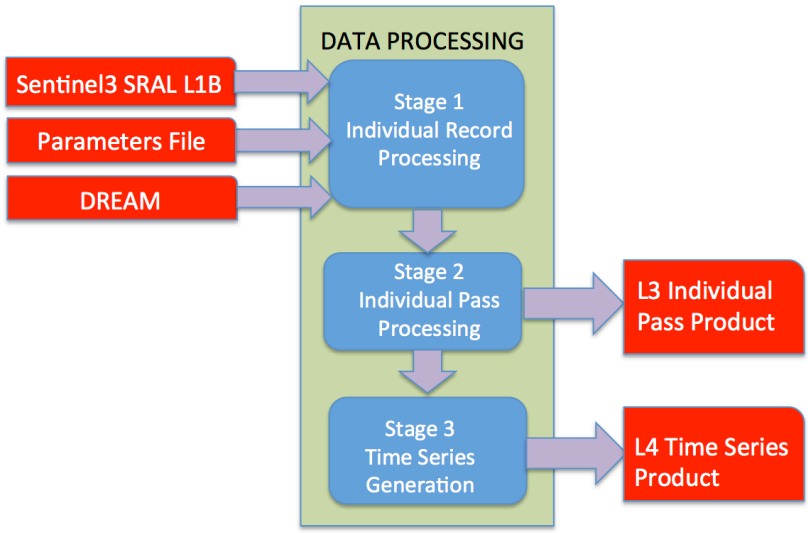


*Figure 31 - Overview of Processing Chain for Sentinel3 Soil Moisture Generation*

#### *3.1.2.2. Assessment*

This section presents results from an assessment of the Cryosat2 derived surface soil moisture estimates (CSME) over the test desert areas. Very limited in-situ data are available for comparison (LOTUS D4.5, 2015). The primary validation dataset utilised was therefore Jason2 derived soil moisture estimates previously discussed.

Track based estimates were used, to minimise the effects of high frequency variations in surface backscatter incompletely captured in the DREAMs. The outcome of this validation was extremely good for the CSME data over both the Kalahari and Tenere deserts, with identification of soil moisture seasonal signatures, which agreed in both phase and magnitude with the Jason2 estimates (Berry & Balmbra, 2015a; 2015b).

For illustration, Jason2 repeat arc locations are shown here for the Tenere enhanced DREAM inFigure 32: the CSME data are shown in Figure 33 together with the Jason2 time series 'bracketing' the spatially disparate CSME track based soil moisture estimates. A more detailed analysis utilising

reduced spatial averaging is now being undertaken, to achieve closer spatial alignment between the Jason2 and Cryosat2 measurements.

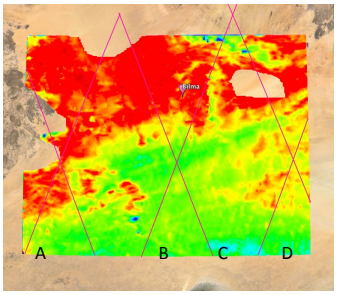


*Figure 32 - Tenere desert DREAM with Jason2 track locations*

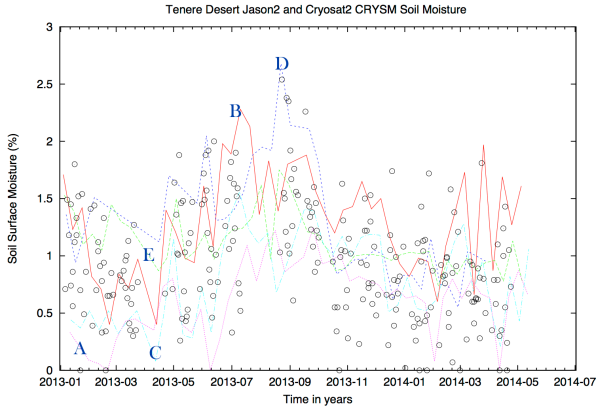


*Figure 33 - Soil Moisture product (CSME) validation with Jason2 soil moisture measurements from tracks in Figure 32 (from Berry & Balmbra, 2015b)*

Similarly good results were obtained for the Kalahari desert. Again, the Jason2 spatially widely separated timeseries 'bracketed' the intervening Cryosat2 track averaged soil moisture estimates, which showed a very clear annual signature. Work is ongoing to reduce the track averaging utilised for both Jason2 and Cryosat2 data over the Kalahari, in order to provide more nearly spatially coincident data, now that the high quality of the recast DREAM is established.

For the Simpson desert, the extremely sparse and aperiodic precipitation, together with the lack of surface drainage, meant that insufficient signals were detected in both datasets to demonstrate correlation, although the results were in agreement. Whilst the lack of surface drainage minimised the chance of residual paleo-hydrology contamination in the Simpson DREAM, this was outweighed by the requirement to detect signals. It was concluded that a much longer time series would be required for CSME validation over this desert.

Taken together with the outcome of the SAR-LRM mode study (Berry & Balmbra, 2015a; 2015b) it was concluded that this technique for soil moisture derivation would work effectively for both Sentinel3 LRM and SAR mode data.

The very good results obtained from building the enhanced DREAMS demonstrate that enhancing the DREAMS over all other desert areas for which DREAMS exist will permit soil moisture products from Sentinel3 to be generated for the Arabian, Gibson, Kalahari, Simpson, Tenere and Victoria deserts. Additionally, the majority of the vast Sahara desert can be modelled, as sufficient ground truth has now been obtained to allow the enhanced Cryosat2 DREAMcrafting to be applied to these deserts. The next step is to include third party data, to allow generation of DREAMS over wetter areas. Here, Cryosat2 has a role, as the long repeat orbit allows extensive testing of each new DREAM prior to use for Sentinel3 product generation.

Whilst track averaged values were produced for the Cryosat2 data CSME products, further assessment and testing have shown that the high spatial along-track averaging applied in the first generation of CSME products is not required. Multiple timeseries are now being generated along each Jason2 arc over the test deserts, and augmented CSME products are being derived from the Cryosat2 data. It is clear that multiple products can be created along each Sentinel3 arc that crosses a DREAM, allowing finer spatial sampling than current remote sensing techniques permit. Estimating for Sentinel3 from prior ERS2 analysis (Berry et al., 2012), together with the Jason2 and Cryosat2 development during the LOTUS project (Berry & Balmbra, 2014; Berry & Balmbra, 2015a;b) gives conservative spatial sampling estimates for soil moisture generation every 18” – 27” along-track over all DREAM regions. This compares with 0.25 degree pixel size for the best current soil moisture estimates using active and passive remote sensing techniques (Wagner et al., 2012). The tradeoff is in the temporal sampling, constrained for satellite altimetry by the orbit repeat pattern. Sentinel3 soil moisture products thus offer unique and complementary datasets to those from other sensors, offering detailed along-track profiles of measurements over large areas.

#### *3.1.2.3. Assumptions and limitations*

The following assumptions were made in the design of the processing chain:

1. An enhanced Cryosat2 recast DREAM model is available, already masked for exclusion criteria, together with its associated parameters file. It is noted that significant amounts of Sentinel3 SAR mode data will be required to calculate Parameter File List characterisation values for the SAR waveforms.

#### *3.1.2.4. Product Structure and Content*

The Level 2 product was not released as individual measurements from Cryosat2 were found to be responding to short wavelength fluctuations in terrain surface roughness and composition, not fully modelled in the DREAMS (Berry & Balmbra, 2014; LOTUS D6.3, 2015).

A Level 3 product was released, for individual tracks of Cryosat2 data, due to the long repeat cycle. This is the CSME dataset.

Each LOTUS CSME Demonstration Dataset contains a space delimited ascii text file. Each dataset comprises two header files, and a datafile containing surface soil moisture estimates derived from the Cryosat2 altimeter. Currently, all desert regions are overflown in LRM mode. Data have been generated for a period of one year from 01/01/2013 to 31/12/2013 for all test areas.

### *(i) CSME Header 1*

The first product header gives information on the data origin (altimeter mission identifier) and the version of the processing scheme used to generate the product. Information on the data originator, data generation date and the region identifier are also given. The header structure is summarized in Table 10.

*Table 10 - Content of CSME Dataset Header 1*

| | |
|---|---|
| Altimeter (CryoSat-2) and mode of operation (SAR or LRM) | Text fields |
| Pre-processorversion and revisión numbers | Text fields |
| CSME processor version | Text field |
| Desert identifier | Text field |
| Data originator and project | Text fields |
| Creation date | Date field dd/mm/yyyy |

### *(ii) CSME Header 2*

This header contains the following information on data content.

*Table 11 - Content of CSME Dataset Header 2*

| | |
|---|---|
| Name of desert region | Text field |
| Data location information | Text field |
| Time field information | Text field |
| Input record information | Text field |
| Soil moisture field information | Text field |

### *(iii) CSME Dataset*

Table 4 shows the fields included in the LOTUS Cryosat2 soil moisture demonstration product. Each estimate is an averaged value along an arc of the satellite overpass. The start and stop locations for the arc used to generate the soil moisture estimate are given, together with the number of points used to form the estimate. It is noted that the current protocol of averaging each overpass to yield one value of soil moisture should be relaxed following further enhancements to the DREAMs (LOTUS D6.3, 2015).

*Table 12 - Content of CSME surface Soil Moisture Dataset*

| Parameter | Unit |
|---|---|
| Segment start Latitude | Decimal degrees |
| Segment start Longitude | Decimal degrees |
| Segment end Latitude | Decimal degrees |
| Segment end Longitude | Decimal degrees |
| Date at centre of track segment | Year / Month / Day |
| Fraction of day at centre of track segment | Hour / Minute / Second |
| Number of points used to form estimate | None |
| Soil moisture mean estimate | Percent surface soil Moisture |

### 3.1.3. Snow depth

#### *3.1.3.1. Major improvements using SAR altimetry*

##### *(i) CryoSat-2*

Firstly, the study started with CryoSat-2 SAR data. The analysis started with a pre-processing phase, where data were collected and calibrated in order to obtain power watts values. Over the two dataset used for the study data covering the 2011, 2012 and 2013 season have been found, a total of about 7000 measurements has been selected.

Additionally the OCOG retracker has been implemented and run over the selected points.

The analysis started studying the correlation between mean power values and snow depth changes, followed by an investigation of the waveforms shapes. As final step a data statistic of the mean power, and OCOG parameters was for each month of the analysed period has been done.

General conclusions:

- It has been found in this study that the waveform total power, OCOG amplitude/area, do not show any trend or relationship with changes in the snow depth.

- The only parameter considered in this analysis with a correlation equal to 0.64 with the snow depth is the OCOG width parameter, on Area 2, for years 2011 and 2012, as shown in figure 34.

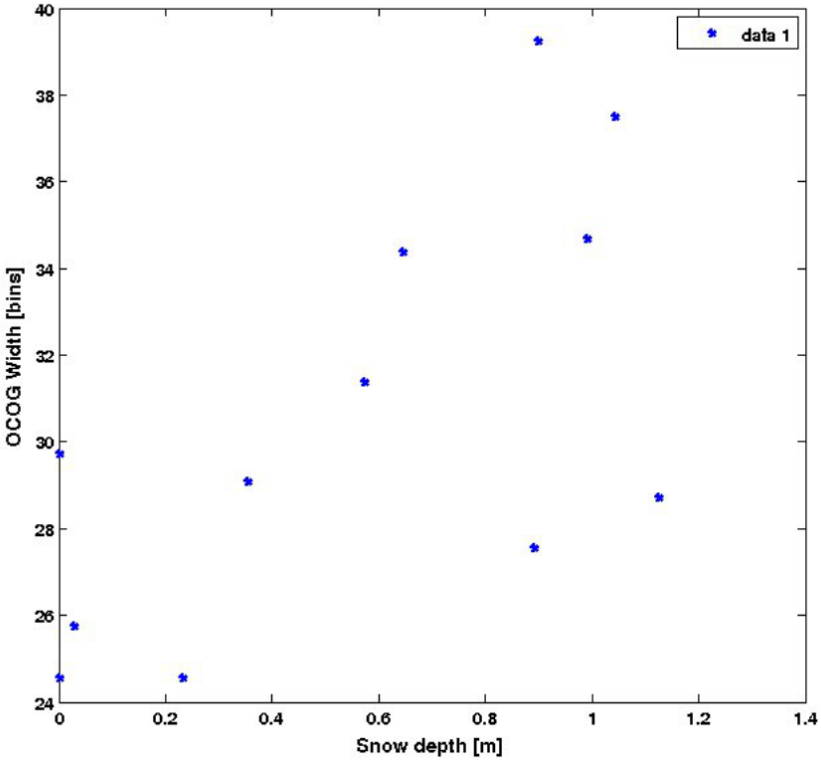


*Figure 34 - OCOG width vs snow depth variations*

- In any case, the correlation found is too weak to develop an operation snow depth retrieval algorithm based on these parameters.

- The reason we find for this, is that the geometry of the observations changes significantly between sequential observations of the same area, due to the fact that the CryoSat-2 orbit is not a repeat pass orbit. Therefore, the topography and changes in the terrain can have important effects on the echo returns can have a stronger impact than any other geophysical parameters.

- We believe this could be different in the case of Sentinel-3, as in this case the satellite will have a monthly repeat pass orbit, that could potentially allow the application of change detection techniques, to mitigate the effect of geometry and topography.

### *(ii) EnviSat*

Secondly, as the Cryosat-2 satellite does not have a repeat track, the study continued with EnviSat data to assess the potential of using sentinel-3 altimeter data (with a repeat pass of 27 days). It was concluded that ENVISAT RA-2 (with a similar repeat pass), could be used for such type of study despite the low resolution. In the following a description of the dataset used, methodology employed, and results will be detailed.

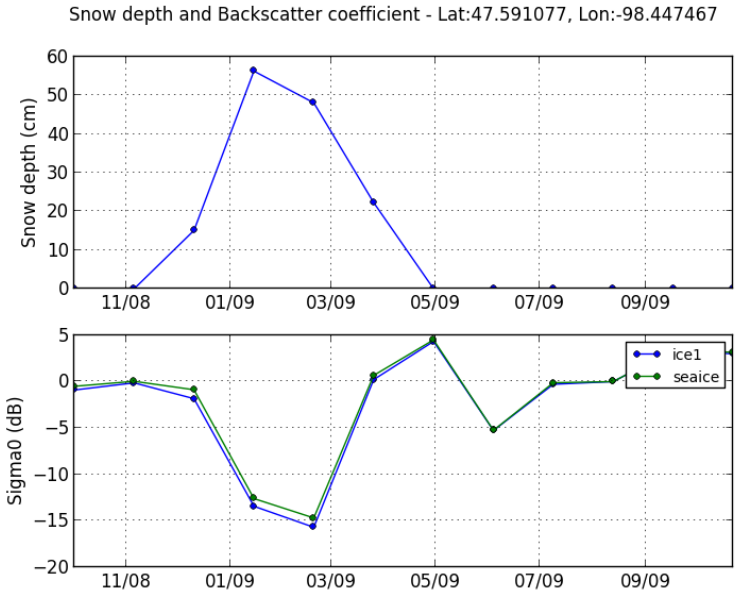


*Figure 35 - Snow depth (up) vs backscatter values (down) for a measurement point over the period Oct. 2008 – Oct. 2009*

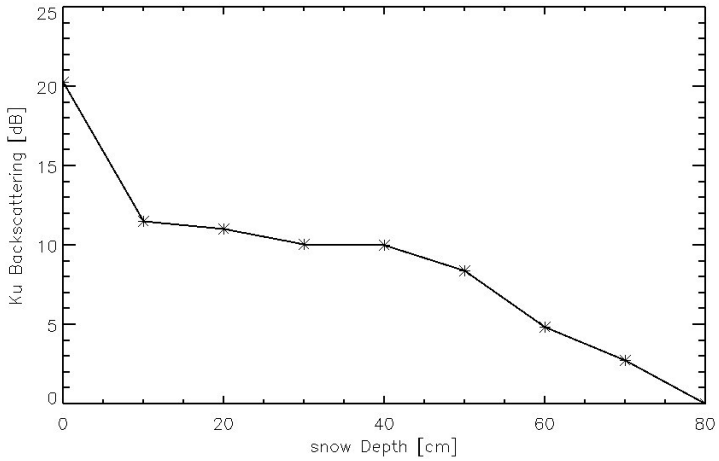


*Figure 36 - Snow-depth vs backscatter values at Ku-band for the whole dataset.*

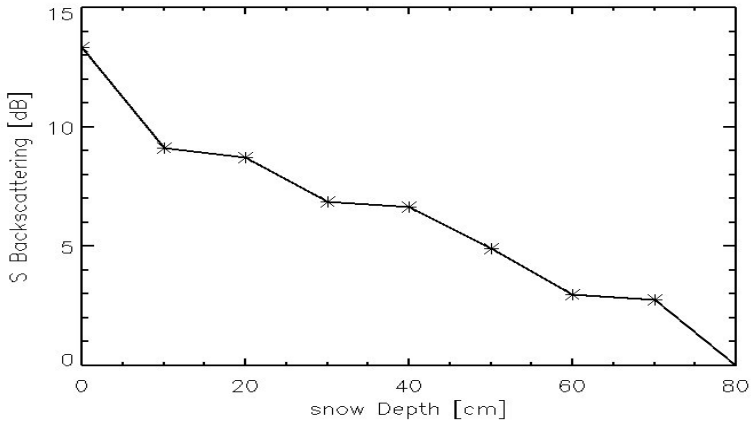


*Figure 37 - Snow-depth vs backscatter values at S-band for the whole dataset.*

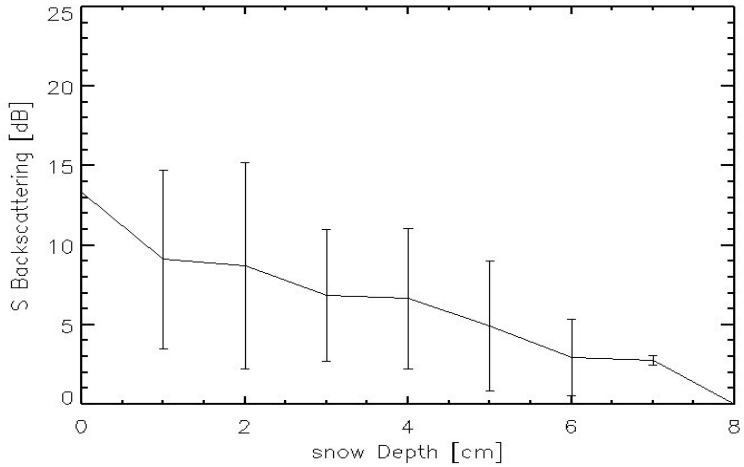


*Figure 38 - Snow-depth vs backscatter values at S-band with std of each bin*

Following the study done with Cryosat-2 data and presented in [D-2.6], a further analysis was done using ENVISAT RA-2 data to assess the potential of using sentinel-3 altimeter data for snow-depth retrieval. The area chosen for the investigation was located in U.S. over the Northern Great plain. The choice was mainly guided by the flat topography, abundance of snow in winter, and presence of ground truth data. Over the areas of interest have been found ENVISAT RA-2 data covering the period between January 2005 and December 2009. About 16500 measurements have been selected over the Area of study. Results showed a clear attenuation as the depth increases, however it looks that there is a big spread of the measurements corresponding to a given snow-depth. This could be due to the large footprint of ENVISAT RA due to the fact that the snow condition can vary within the illuminated area. We believe this could be different in the case of Sentinel-3, as in this case the satellite will have a higher resolution that could potentially allow a better filtering of the waveforms.

#### *3.1.3.2. Products*

The snow depth estimation from SAR altimetry stayed at research level. Several results suggest the possibility to use SAR altimetry for snow depth estimation. However, the advancement is not enough mature to provide an algorithm able to produce snow depth products.

## 3.2. Recommendations

### 3.2.1. River and lakes

In this project we have demonstrated the grate potential of SAR altimetry for inland water. Compared to conventional altimetry, the derived water levels for the individual crossings are significantly more stable. Despite the smaller footprint in the along-track direction the waveform can still be affected by signals from the surrounding land, which might lead to incorrect water level estimates. To handle this sub-waveform retrackers and retrackers that consider multiple peaks have been tested, with positive results. However further research is recommended.

The drifting track pattern of CryoSat-2 brings benefits but also challenges. On the positive side a significantly larger amount of lakes are visited, which can lead to new interesting results. The drifting track pattern of CryoSat-2 causes the tracks to cross the water bodies at different locations. For lakes the problem is lesser, since a lake can be considered a closed system. However, we might introduce errors eg a geoid error into the water level time series. For rivers, which are not confined to a specific elevation, it is more challenging to derive water level time series at virtual stations, since the surface elevation is a function of both space and time. Hence, to derive water level time series at virtual stations additional information is needed. This could be a highly accurate digital elevation model. In areas with gently sloping terrain a linear slope correction can be used to account for the terrain. This approach has been applied successfully in this project.

Sentinel-3 will operate in a 27 day repeat orbit and will therefore not be challenged by the issues mentioned above.

### 3.2.2. Soil moisture

The ESA SMALT project has already demonstrated generation of soil moisture products from satellite radar altimetry. As this methodology continues to mature and the DREAMS become more precise and encompass larger areas, operational products are foreseen. The automated processing is already well defined and it is probable that products could be operationally generated within 1-2 years of data acquisition from Sentinel3. This allows time to rebuild the DREAMS incorporating assessment from repeat cycles of Sentinel3 SRAL altimetry.

Clearly one key question must be answered: to what extent can the spatial averaging constraint be relaxed? Land surfaces (apart from water in liquid or solid form, and salars) are poor reflectors of Ku band nadir illumination; thus the effective footprint (that part of the surface contributing significantly to the returned echo) is far smaller than the pulse-limited footprint even for conventional altimeters. This is further constrained in the along-track direction for SAR altimetry. If the prediction of soil moisture products every 18” to 27” is realised (and possibly exceeded as SAR altimetry should permit less spatial averaging) then altimeter soil moisture products would provide a far finer spatial sampling

along-track than other remote sensing techniques, although at reduced temporal sampling. However, the precision of altimeter backscatter measurement can be of order 0.1dB, allowing very precise estimates of soil moisture to be made. The foreseen role for this product is thus complementary to that of other remote sensing techniques.

### 3.2.3. Snow depth

The estimation of snow depth using altimeter is not enough mature yet to develop operational products. But, through the investigation, interesting results shows a trend in the data that could allow snow depth estimation. However, it looks that the measurements corresponding to a given snow-depth are spread. This could be due to the large footprint of ENVISAT RA due to the fact that the snow condition can vary within the illuminated area. We believe this could be different in the case of Sentinel-3, as in this case the satellite will have a higher resolution that could potentially allow a better filtering of the waveforms.

## 4. Reference

LOTUS Deliverable D1.3: SAR mode for Ocean Algorithms Theoretical Basis Document

Berry, P.A.M. & Balmbra,R., 2015a. Surface Soil Moisture From Satellite Altimetry - From Cryosat2 To Sentinel3. Proceedings ESA Sentinel3 for Science Workshop, June 2015. In press.

Berry, P.A.M. & Balmbra, R., 2015b. Surface Soil Moisture from SRAL Satellite Radar Altimetry. Proceedings, ESA Third Space for Hydrology Workshop, September 2015, in press.

Berry, P.A.M. & Balmbra, R., 2014. D 2-4 Cryosat2 Soil Surface Moisture Algorithm Theoretical Basis Document. http://www.fp7-lotus.eu/Publications/Deliverables/

Berry, P A. M. & Carter, J.O., 2010. Cross Calibration of SMOS Soil Moisture Measurements with Satellite Radar Altimetry Estimates and In-Situ Data. Proceedings of ESA Living Planet Symposium, ISBN 978-92-9221-250-6.

Berry, P.A.M., Carter, J.O., 2011. Altimeter derived Soil Moisture Determination – Global Scope and Validation. IAHS 'red book' for IUGG 2011

Berry, P.A.M., Dowson, M., Smith, R.G., Benveniste, J., 2012. Soil Moisture From Satellite Radar Altimetry (SMALT). Proceedings of the ESA Living Planet Symposium 2012.

Bramer, S.M.S. & Berry, P.A.M. 2010. Soil Surface Moisture From EnviSat RA-2: From Modelling Towards Implementation. P205-212, International Association of Geodesy Symposia, Vol. 135, ISBN: 978-3-642-10633-0.

ESA SMALT Project website: http://tethys.eaprs.cse.dmu.ac.uk/SMALT/ accessed March 2014

LOTUS D6.3, 2015. Soil moisture downstream added value services. Submitted.

LOTUS D4.5, 2015. Report describing results from the assessment of the prototype datasets. Submitted.

Wagner, W., W. Dorigo, R. de Jeu, D. Fernandez, J. Benveniste, E. Haas, M. Ertl , 2012. Fusion of active and passive microwave observations to create an Essential Climate Variable data record on soil moisture, ISPRS Annals of the Photogrammetry, Remote Sensing and Spatial Information Sciences (ISPRS Annals), Volume I-7, XXII ISPRS Congress, Melbourne, Australia, 25 August-1 September 2012, 315-321.

[END OF DOCUMENT]